

In presenting the dissertation as a partial fulfillment of the requirements for an advanced degree from the Georgia Institute of Technology, I agree that the Library of the Institute shall make it available for inspection and circulation in accordance with its regulations governing materials of this type. I agree that permission to copy from, or to publish from, this dissertation may be granted by the professor under whose direction it was written, or, in his absence, by the Dean of the Graduate Division when such copying or publication is solely for scholarly purposes and does not involve potential financial gain. It is understood that any copying from, or publication of, this dissertation which involves potential financial gain will not be allowed without written permission.

7/25/68

LOW CYCLE FATIGUE TESTING OF LOW CARBON STEEL

A Thesis

Presented to

The Faculty of the Graduate Division

by

Frank Wu Sun

In partial fulfillment

of the Requirements for the Degree

Master of Science in Mechanical Engineering

Georgia Institute of Technology

May 1971

LOW CYCLE FATIGUE TESTING OF LOW CARBON STEEL

Approved:

Chairman

(Signature)

Date:

May 21, 1971

TABLE OF CONTENTS

	Page
ACKNOWLEDGMENTS.....	111
LIST OF TABLES.....	iv
LIST OF ILLUSTRATION.....	v
NOMENCLATURE.....	vii
SUMMARY.....	ix
Chapter	
I. INTRODUCTION.....	1
II. DISCUSSION OF LOW CYCLE FATIGUE.....	3
Cyclic Hardening, Softening and Intermediate State	
Hysteresis Loop	
Cyclic Stress-Strain Curve	
Cyclic Strain Hardening Exponent	
Hysteresis Loop Area and Plastic Energy	
Stress Amplitude-Number of Reversals Curve	
Fatigue Ductility Properties	
Fatigue Strength Properties	
Resistance To Total Strain	
Plastic Energy Per Cycle	
Total Energy Required for the Fatigue Fracture	
III. SPECIMEN AND EQUIPMENT DESIGN.....	18
Specimen Design	
Fixture Equipment Design	
Comparison of Equipment Used for Low Cycle Fatigue Tests	
IV. OPERATION, DATA AND RESULTS.....	27
Strain Measurement and Control	
Data and Results	
V. CONCLUSION AND RECOMMENDATIONS.....	30
BIBLIOGRAPHY.....	56

ACKNOWLEDGMENTS

The author is indebted to the individuals who have contributed to the success of this work. In particular, he would like to express his appreciation to his Thesis Advisor, Dr. John H. Murphy, for his valuable guidance throughout this study. He would also like to thank Dr. William R. Clough and James Ting-Shun Wang for their fruitful suggestions and discussions. An extreme debt of gratitude is owed to the National Science Council of the Republic of China which gave the author a fellowship of two years to study in the United States. The author also wishes to extend his heartfelt thanks to Mr. Raymond G. Grim for producing the experimental equipment and test specimens.

The author would like to express his sincere appreciation to his parents for their loving guidance and to his wife for her love, patience, and understanding.

LIST OF TABLES

Table	Page
1. Fatigue Properties of 1018 Cold Worked Steel.	28
2. Half Life Cyclic Stress and Plastic Strain at Several Constant Strain Amplitude Tests.	28

LIST OF ILLUSTRATIONS

	Page
1. Illustration of Cyclic Hardening and Cyclic Softening	33
2. Hysteresis Loop at Stable Condition	34
3. Hysteresis Loop Converted to Stress-Plastic Strain Relation from Stress-Strain Plot	34
4. Illustration of Plastic Energy Calculation.	35
5. Illustration of Cyclic Stress-Strain Curve Established by Multiple Step Tests.	35
6. Cyclic Stress-Strain Curve Established by Incremental Step Tests.	36
7. Cyclic Stress-Strain Curve Established by Incremental Step Tests.	37
8. Cyclic Stress-Strain Curve Established by Monotonic Tension	38
9. (A) Comparison of Monotonic Stress-Strain Curve and Cyclic Stress-Strain Curve (Cyclic Softening Material).	39
(B) Comparison of Monotonic Stress-Strain Curve and Cyclic Stress-Strain Curve (Cyclic Hardening Material).	39
(C) Illustration of Plastic Strain Hysteresis Loop on the log-log Scale	39
10. σ_a - 2N Curve of 1018 Cold Worked Steel	40
11. Plastic Strain Energy as a Function of Number of Reversals.	41
12. Cyclic Stress-Plastic Strain Line on a log-log Scale.	42
13. Fatigue Ductility Properties.	43
14. Fatigue Strength Properties	44
15. Total Cyclic Strain-Life in Reversals	45
16. Plastic Energy per Cycle-Life in Reversals.	46

LIST OF ILLUSTRATIONS (Concluded)

	Page
17. Total Plastic Energy-Life in Reversals.	47
18. Specimen Dimensions	48
19. Assembly View of Reversed-axial-load Test Equipment (Fixed-pinned End).	49
20. Assembly View of Reversed-axial-load Test Equipment (Fixed-fixed End)	50
21. Dimensions of Equipment Parts	51
22. Dimensions of Equipment Parts	52
23. Dimensions of Equipment Parts	53
24. Specimen Modification	54
25. A Brief Circuit of Automatic Control System	55

NOMENCLATURE

Δe_t	=	total strain range
Δe_2	=	elastic strain range
Δe_p	=	plastic strain range
$\frac{\Delta e_p}{2}$	=	plastic strain amplitude (at the tip of the hysteresis loop)
σ_a	=	stress amplitude (at the tip of the hysteresis loop)
σ	=	stress at a general point in the hysteresis loop
e_p	=	plastic strain at a general point on the hysteresis loop
e_f'	=	fatigue ductility coefficient
e_f	=	true fracture ductility
σ_f'	=	fatigue strength coefficient
σ_f	=	true fracture strength
b	=	fatigue strength exponent
c	=	fatigue ductility exponent
N_f	=	fatigue life; number of cycles to failure
N	=	number of cycles
$2N_f$	=	number of reversals to failure
n'	=	cyclic strain hardening exponent
ΔW	=	plastic strain energy per cycle
W_f	=	total plastic strain energy required to cause fatigue failure
W_f'	=	$4\sigma_f' e_f' \frac{1 - n'}{1 + n'}$ intercept of the $\log \Delta W - \log 2N_f$ line at $2N_f = 1$

- $\frac{1}{2}W'_f = 2\sigma'_f \epsilon'_f \frac{1 - n'}{1 + n'}$
intercept of the $\log W_f - \log 2N_f$ line at $2N_f = 1$
- E = modulus of elasticity
- P_{cr} = the critical load for elastic buckling
- P'_{cr} = the critical load for waved buckling
- K = a constant determined by boundary conditions of Euler column equation
- I = moment of inertia
- l = the calculated length
- A = cross-sectional area of the specimen
- ϵ_{cr} = average strain at instability
- E_s = secant modulus
- E_t = tangent modulus
- γ = radius of gyration
- d_o = outside diameter
- d_i = inside diameter
- t = thickness of the wall of tube shaped specimen

SUMMARY

This thesis discusses the low cycle fatigue and cyclic plastic energy of 1018 cold worked steel under conditions of room temperature and constant total strain range. Total strain ranges varying from 0.04 in/in to 0.008 in/in were used. Fatigue properties such as fatigue-ductility exponent, fatigue-ductility coefficient, fatigue-strength exponent, and fatigue-strength coefficient have been determined. From the hysteresis loops at different constant total strain ranges, the plastic energy per cycle and the total plastic energy to fracture the specimen have been calculated. For 1018 cold worked steel, it has been observed that the cyclic stress always decreases throughout the tests.

Two types of specimen fixtures were designed according to boundary conditions of the Euler column buckling equation. One type grips the specimen in a manner corresponding to fixed-fixed end conditions. The other type gives a fixed-pinned end condition. Both these fixtures satisfy the condition of self alignment.

CHAPTER I

INTRODUCTION

There is a long history associated with experimental determination of the fatigue characteristics of metals and alloys. Unfortunately, the development of applicable theory has lagged far behind. In recent years, there has been an appreciable effort to incorporate low-cycle fatigue data into appropriate design procedures. About eighty years ago, several researchers initiated studies in this field. In 1910, O. H. Basquin (1) presented his famous exponential law of endurance tests after extensive study of existing experimental data which included repeated tension, tension and small compression, beam rotation under bending load, and simple reversed bending. These data were all obtained under constant load amplitude conditions.

In 1953, L. F. Coffin (2) developed an empirical equation which expressed the fatigue life as a function of plastic strain range under constant strain. However, in 1964, JoDean Morrow (3), having studied the fatigue properties of several materials, established an expression which verified that the total plastic energy required to fracture the specimen increases as the fatigue life increases.

In the work reported in this thesis, there were performed on 1018 cold worked steel a series of constant strain range tests which produced fatigue lifes varying from a few reversals ($2N_f$) to several thousand reversals. The specimens were subjected to axial-load completely

reversed strain amplitude cycling. Cyclic stress amplitude was measured periodically throughout the tests. From these data the following fatigue properties were investigated: the cyclic strain hardening exponent, the stress amplitude-number of reversals relationships, fatigue ductility properties, fatigue strength properties, total cyclic strain amplitude as a function of reversals, plastic strain energy per cycle, and the total plastic energy required to fracture the specimen.

The following low cycle fatigue properties of 1018 cold worked steel were obtained: fatigue ductility coefficient $\epsilon_f' = 0.16$ in/in, fatigue ductility exponent $c = 0.537$, fatigue strength coefficient $\sigma_f' = 88,500$ psi, fatigue strength exponent $b = 0.0805$, cyclic strain hardening exponent $n = 0.15$, and transition life $2N_t = 6,800$ R.

Two types of loading fixtures were designed for testing the tension-compression specimens by means of the Instron Machine installed in the School of Mechanical Engineering, Georgia Institute of Technology. One type gripped the specimen in a manner corresponding to fixed-fixed end condition. The other type gave a fixed-pinned end condition. Both fixtures were designed to satisfy the condition of self alignment.

CHAPTER II

DISCUSSION OF LOW CYCLE FATIGUE

Cyclic Hardening, Softening and Intermediate State

Cyclic hardening, cyclic softening and the intermediate state may occur in completely reversed axial-load tests. Under the constant strain condition a specimen is first subjected to a tensile load which produces a total strain OA in the plastic region, but not beyond the strain corresponding to the ultimate strength, as shown in Figure 1. This process is expressed by the curve Oa , which is the initial part of the engineering stress-strain curve in a monotonic increasing tensile test. When the specimen is unloaded, a straight line ab having a slope parallel to the elastic line is traced.

Subsequently, the specimen undergoes a compressive load to a strain OC which is equal to OA in magnitude. When another unloading process is imposed on the specimen, a straight line, de , with a slope parallel to the elastic line will be produced. Finally, the specimen is again subjected to a tensile loaded process until the initial strain OA is reached; thus, a complete testing cycle is established.

In the above testing cycle, OA represents the total strain amplitude, Ob the plastic strain amplitude, and bA represents the elastic strain amplitude. The total strain range is CA .

During an axial-load low cyclic fatigue test, the above cycle will be repeated many times from a few to several thousand cycles. If the total strain range is kept constant, the cyclic stress, P/A (or

deformation resistance) will change as the number of cycles increases. If the deformation resistance of the specimen increases during the test, this characteristic is termed cyclic hardening. If the deformation resistance decreases during the test, the behavior is called cyclic softening. If the deformation resistance changes slightly (alternatively increases and decreases) or remains unchanged, we term this material as being in an intermediate state.

If the testing condition is changed to a constant load condition, the total strains will change with the number of the testing cycles. If the total strain amplitude increases with the increase of testing cycles, we term this behavior as cyclic softening. In this condition, the deformation resistance becomes weaker and weaker. If the total strain amplitude decreases with the increase of testing cycles, we term this characteristic as cyclic hardening. In this condition, the deformation resistance becomes stronger and stronger.

Hysteresis Loop

During the constant strain amplitude test, the rate of change of deformation resistance is large during the early few cycles of the tests. However, it will diminish and reach approximately a stable condition in the following cycles. When the deformation resistance reaches an approximately stable condition, a loop shaped curve is formed on the stress-strain plot; this is called the hysteresis loop and is as shown in Figure 2. From the hysteresis loop, we establish an equation as follows:

$$\Delta \epsilon_t = \Delta \epsilon_e + \Delta \epsilon_p \quad (2-1)$$

$\Delta\epsilon_t$ is the total strain range which can be obtained from the load-elongation recorder on the testing machine. $\Delta\epsilon_e$ is the elastic strain range which can be calculated from the expression $\frac{2\sigma_a}{E}$, where σ_a is the stress amplitude corresponding to the given strain amplitude in a constant strain range test. The testing region is general between the yield point (0.2% off set) and up to 7 times of the yield strain. From the plasticity theory, the expression $\frac{2\sigma_a}{E}$ can be used to obtain the elastic strain range in this region. The difference, $\Delta\epsilon_t - \Delta\epsilon_e$, is the plastic strain range term which will be used to explore the fatigue ductility properties of 1018 cold worked steel.

In the calculation of $\Delta\epsilon_e$, the engineering stress is used since, in this testing region, the difference between the true stress and engineering stress is very small and may be neglected.

For a cold worked material, such as 1018 cold worked steel, the deformation resistance always decreases under constant strain range testing condition. The hysteresis loop seems never to reach a stable condition (see Figure 10)--it will continue to soften just prior to fatigue fracture.

The plastic strain range is the width of the hysteresis loop. Comparing Figure 1 and 2, we see that the plastic strain range has a tendency to decrease for a cyclic hardening material during the tests. For a cyclic softening material, especially 1018 cold worked steel, the plastic strain range always increases during the tests. Therefore, the plastic strain range value at the half life cycle is adopted in the calculation of fatigue ductility properties.

Cyclic Stress-Strain Curve

In low cycle fatigue tests the hysteresis loops change rapidly in the first few cycles of testing. As long as control conditions are not altered, the tested material will gradually reach a stable condition which may be observed roughly from the hysteresis loops. If fatigue tests are conducted using the same shaped specimens and the tips of the stable loops are connected from several companion tests at different strain ranges, a smooth curve is obtained. This curve is called the cyclic stress-strain curve which can be determined by one of the following methods.

(1) Connecting the tips of hysteresis loops at the half life

The cyclic stress-strain curve may be obtained by connecting the tips of several hysteresis loops which are picked up from the middle loops of the fatigue life tests on a group of identically shaped specimens. The fatigue life tests are conducted in completely reversed axial tension-compression, but at different strain amplitudes. Figure 9(A) shows the cyclic stress-strain curve of 1018 cold worked steel. The coordinates of six points on this curve are the corresponding cyclic stress and strain amplitude of half life value.

(2) Multiple step tests

Since the hysteresis loop approaches a stable condition quite quickly, after a sudden change in cyclic strain amplitude (4), it is possible to obtain several points from the same specimen tested at different strain ranges. This method of determining the cyclic stress-strain curve is very convenient and the curve can be justified. Figure 5

is an illustration of this method. The hysteresis loops on this figure are at different stable conditions. Through the tips of these hysteresis loops, the cyclic stress-strain curve are drawn.

(3) Incremental step tests

This method of determining the cyclic stress-strain curve consists mainly of gradually increasing the strain amplitude until the cyclic strain amplitude reaches about $\pm 2\%$ (4). Then the strain amplitude is gradually reduced again, and the procedure repeated until the cyclic stress-strain curve is stabilized. The cyclic stress-strain curve is traced through the tips of the individual hysteresis loops.

This method has been performed on the testing machine by the author. The tested material is 1018 cold worked steel. The first step is shown in Figure 6(A). Starting with a virgin specimen, the cyclic strain amplitude is gradually increased until ± 0.02 in/in strain amplitude is reached. An interesting phenomenon occurs in cyclic softening materials; the deformation resistance becomes weak very rapidly in the cyclic test. The decrease of the cyclic stress continues even under the condition of increase of the cyclic strain amplitude.

Figure 6(B) indicates the second step of this procedure. The cyclic strain is gradually decreased to zero (since the zero point is very hard to get, the procedure may be stopped at the nominally elastic region).

Figure 7(A) shows the third step. The strain is cyclically increased again to the maximum strain amplitude ($\pm 2\%$). It should be noted that the deformation resistance is approximately at a stable condition.

Figure 7(B) indicates the final step of this method. The strain is gradually decreased again. Comparing it to Figure 7(A), it is clear that the deformation resistance at every tip is approximately equal to that in Figure 7(A). Through these tips of individual loops, a cyclic stress-strain curve can be drawn.

(4) Monotonic tension after incremental step tests

There is another method for obtaining the cyclic stress-strain curve. After the increasing-decreasing-increasing-decreasing incremental strain cycling, the specimen is pulled to fracture in tension (4). This is an advantageous way to establish the cyclic stress-strain curve because only one tension need be imposed on the specimen which was just employed in the incremental step tests. As shown in Figure 8, this curve, compared to the cyclic stress-strain curve determined by other means, is a little lower at high strains.

From the phenomenon of cyclic hardening and softening, and the method of "connecting the tips of hysteresis loops at the half life" to get the cyclic stress-strain curve, we may state that the cyclic stress-strain curve will be above the monotonic curve for metals which are cyclic hardening, and the cyclic stress-strain curve will be below the monotonic curve for metals which are cyclic softening. Figure 9(A) shows a 1018 cold worked steel which has a cyclic softening behavior. Figure 9(B) shows waspaloy BK (3) having a cyclic hardening behavior.

Cyclic Strain Hardening Exponent

If we discard the elastic part of the cyclic stress-strain curve, the cyclic stress-plastic strain curve will be established. It is not necessary to construct the cyclic stress-plastic strain curve on an arithmetic scale since this gives no help in the analysis of fatigue properties.

Figure 12 shows the cyclic stress-plastic strain curve of 1018 cold worked steel on a log-log scale. On this plot, it is a straight line. Several points on this line were obtained from the half life value of stress amplitude and plastic strain amplitude as shown in Table 2. If we plot the fatigue strength coefficient and the fatigue ductility coefficient on this diagram, their values will be a point on this line. Thus, an empirical equation is established:

$$\frac{\Delta \epsilon_p}{2} = \epsilon_f' \left(\frac{\sigma_a}{\sigma_f'} \right)^{1/n'} \quad (2-2)$$

The slope of this line n' is called the cyclic strain hardening exponent. The value of n' is surprisingly close to being a constant in the neighborhood of 0.15 for most metals. (4)

Hysteresis Loop Area and Plastic Energy

The area of the hysteresis loop represents the plastic strain energy dissipated per cycle. Figure 2 illustrates a hysteresis loop on a stress-strain plot. In calculating the plastic energy per cycle, it is best to discard the elastic range and deal solely with the plastic range. Figure 3 illustrates a geometric method of converting the hysteresis loop from stress-strain to stress-plastic strain relation.

If we plot the hysteresis loop in stress-plastic strain relation on a log-log scale, it will appear as a straight line. JoDean Morrow found that the slope of this line is very approximately equal to n' which was previously defined as the cyclic strain hardening exponent. This may not be strictly correct, but it is a good approximation to use n' to predict the plastic energy dissipated per cycle. On the other hand, we observe in Figure 5 that the geometric shape of the part of OA on the cyclic stress-strain curve is similar to that of A'A on the hysteresis loop. The difference between these two curves is only that the curve A'A is twice that of OA in geometric shape. Thus, it is reasonable to take $n = n'$ in the calculation of the plastic energy from the hysteresis loop. Figure 9(C) shows a stress-plastic strain hysteresis loop plotted on a log-log scale from which an empirical equation is obtained:

$$\epsilon_p = \Delta\epsilon_p \left(\frac{\sigma}{2\sigma_a} \right)^{1/n'} \quad (2-3)$$

where ϵ_p is a plastic strain measured from 0 in Figure 4.

In low cycle fatigue testing, the specimen is first given a tensile stress beyond the yield point and then loaded with a compressive stress. For a cold worked material specimen, the Bauschinger effect will occur (5). The compressive stresses (at the lower tips of hysteresis loops) are smaller than the tensile stresses (at the top tips of hysteresis loops) during the first few cycles of the constant strain range test. If the hysteresis loops gradually approach an approximately stable state, the tensile and compressive stresses will

reach a condition of an equal magnitude. That is to say, the mean stress will be equal to zero and the hysteresis loop will be symmetric with respect to the origin.

Stress Amplitude-Number of Reversals Curve

If the specimen is tested under constant strain conditions, the stress amplitude is a function of the number of reversals ($2N$). The $\sigma_a - 2N$ curve may be plotted on a semilog scale. Figure 10 illustrates several $\sigma_a - 2N$ curves at different strain ranges where the tested material is 1018 cold worked steel which is a cyclic softening material. Figure 10 shows that the cyclic stress amplitude decreases with the increase of reversals.

If the tested material is a cyclic hardening material, the cyclic stress amplitude will increase with the increase of reversals. For some cyclic hardening materials, the cyclic stress change may be divided into two cases. If the strain amplitude is large, the stress amplitude first increases and then decreases as the reversal increases. If the strain amplitude is small, the stress amplitude is always increasing during the test.

If, during the constant strain test, we impose a sudden change to the tested specimen, such as the establishment of the cyclic stress-strain curve by multiple step tests, the strain range is changed suddenly from a low to high level. The cyclic stress will increase suddenly and then change gradually as the reversal increases. The $\sigma_a - 2N$ curve will be discontinuous at the reversal where the increase occurred.

Fatigue Ductility Properties

From a series of constant strain range tests, we may calculate the plastic strain amplitude. The plastic strain amplitude and the corresponding fatigue life (in reversals) are then plotted on a log-log scale. Several points are obtained from this diagram. A straight line called the life line may be drawn through these points. The intercept of the life line with one reversal is called the fatigue ductility coefficient, which is very close to the true fracture ductility of the tested material (4). The slope of the life line is called the fatigue ductility exponent. Figure 13 shows the fatigue ductility properties of 1018 cold worked steel. Since the plastic strain amplitude always increases during the test, the half life plastic strain amplitude value should be adopted. From Figure 13, an empirical equation is established as follows:

$$\frac{\Delta \epsilon_p}{2} = \epsilon_f' (2N_f)^c \quad (2-4)$$

If the tested material is changed, the fatigue ductility exponent will be slightly different, and the life line will be displaced upward for more ductile materials and downward for less ductile materials. Equation (2-4) is similar to Coffin's relation (2):

$$N^K \Delta \epsilon_p = c$$

where: $K = 1/2$, but Morrow pointed out that K is not a constant. K corresponding to c in Equation (2-4) is one of the fatigue properties,

the range of fatigue exponent is from -0.5 to -0.7 (3) depending on the tested materials. The constant related to the fracture ductility, c , when compared to Equation (2-4), would be equal to $2\epsilon_f'$

Fatigue Strength Properties

Eliminating $\Delta\epsilon_p$ by combining Equation (2-2) and Equation (2-4) and assuming $n'c = b$, an equation for the fatigue strength is obtained:

$$\sigma_a = \sigma_f'(2N_f)^b \quad (2-5)$$

$$\frac{\Delta\sigma}{2} = \sigma_f'(2N_f)^b \quad (2-6)$$

For most materials, Equation (2-5) appears as a straight line on a $\log \sigma_a - \log (2N_f)$ plot. This line is also called the life line. The intercept of the life line with one reversal is called the fatigue strength coefficient, σ_f' . The slope of the life line is called the fatigue strength exponent which is in the range from -0.07 to -0.09 (3). Some materials may exhibit an "endurance limit" or a stress below which fatigue failure is highly improbable. The life line in Figure 16 will have a knee and become nearly horizontal approximately beyond 10^7 cycles.

In 1910, O. H. Basquin expressed his famous "exponential law of endurance tests" as follows:

$$S = CR^n$$

where: S = maximum stress in tests

C = intercept (corresponding to σ_f' in Equation (2-5))

$n = 0.12$

R = repetition of cycles

Comparing Equation (2-5) and Basquin's exponential law, we see that their form is identical.

In the discussing of cyclic hardening and cyclic softening, it was seen that the cyclic strain would change under constant load tests, and the cyclic stress would change under constant strain tests. For the purpose of analysis of plastic strain energy per cycle, the constant strain range tests were adopted. The life line (solid) in Figure 14 (or Equation (2-5)) was established from the half life stress amplitudes under different constant strain ranges. This condition is different from the condition (constant load) from which Basquin's equation is derived. For the other purpose, to obtain the mean value of elastic strain amplitude in the calculation of total strain, Equation (2-5) is still established under constant strain range and then divided by E. The expression is $\frac{1}{2}\Delta\epsilon_e = \frac{\sigma_a}{E} = \frac{\sigma'_a}{E}(2N_f)^b$. σ_a is the stress amplitude at half cycle.

Resistance to Total Strain

Dividing Equation (2-5) by E, the elastic strain amplitude is obtained in terms of the fatigue strength coefficient, fatigue strength exponent and the fatigue life. Adding Equation (2-4) for the plastic strain amplitude in terms of the fatigue ductility coefficient, fatigue ductility exponent and the fatigue life, we reach

$$\frac{\Delta\epsilon_t}{2} = \frac{\sigma'_f}{E} (2N_f)^b + \epsilon'_f (2N_f)^c \quad (2-7)$$

Equation (2-7) establishes a formula for the total strain amplitude in terms of the fatigue life where σ_f' , b , ϵ_f' and c are fatigue properties of a given material. Thus, they are constants in Equation (2-7).

On a log-log plot, the total strain is plotted as a curved line as shown in Figure 15. The intersection of the line representing the elastic strain term and the line representing the plastic strain term is called the "transition life." At this point, the elastic strain is equal to the plastic strain. On the left of this point the plastic strain is large and on the right the elastic strain is predominant.

Plastic Energy Per Cycle

The plastic energy per cycle is evaluated by using the cyclic strain hardening exponent. The hysteresis loop at half life cycle is traced on the stress-plastic strain plot as illustrated in Figure 4. It is seen that the rectangle area, $\Delta\sigma_a \cdot \Delta\epsilon_p$, minus the two small areas between the loop and the rectangle is the area of hysteresis loop; thus, the hysteresis loop area may be expressed as follows:

$$\Delta W = \Delta\sigma_a \Delta\epsilon_p - \int_0^{2\sigma_a} \epsilon_p d\sigma \quad (2-8)$$

Substituting Equation (2-3) for $\epsilon_p = \Delta\epsilon_p \left(\frac{\sigma}{2\sigma_a}\right)^{1/n'}$ into Equation (2-8) and performing integration and the necessary algebraic operation, we reduce the expression to the following form:

$$\Delta W = \Delta\sigma_a \cdot \Delta\epsilon_p \frac{1 - n'}{1 + n'} \quad (2-9)$$

From the relation $b = n'c$, Equation (2-9) may be expressed as

$$\Delta W = \Delta \sigma_a \cdot \Delta \epsilon_p \frac{c - b}{c + b} \quad (2-10)$$

Thus, the plastic strain energy per cycle for a given stress and plastic strain range is their product times a constant, $\frac{c - b}{c + b}$. By combining Equations (2-10), (2-6), and (2-4), an expression for the plastic energy per cycle involving the fatigue life is established,

$$\Delta W = 4\sigma_f' \epsilon_f' \frac{c - b}{c + b} (2N_f)^{b+c} \quad (2-11)$$

Equation (2-11) is plotted on a $\log \Delta W - \log (2N_f)$ diagram as shown in Figure 16, and is a straight line (3). The term, $4\sigma_f' \epsilon_f' \frac{c - b}{c + b}$, represented by W_f' is the intercept at one reversal. The term $b + c$ is the slope of the line. The plastic strain energy per cycle will decrease as the number of reversals to fracture the specimen increases.

It should be noted that the dashed lines on Figure 11 will approximately represent Equation (2-11). The dashed line passing through the half life values is incorrect to the life in reversal, and the line passing through the break points is incorrect to the intercept, $4\sigma_f' \epsilon_f' \frac{c - b}{c + b}$.

Total Energy Required for the Fatigue Fracture

Since the plastic energy dissipated per cycle is nearly constant throughout the fatigue tests, as shown in Figure 11, the total plastic energy to fracture the specimen can be approximated (3) by $W_f = \Delta W N_f$. Substituting Equation (2-11) into the above equation, we obtain

$$W_f = W'_f(2N_f)^{b+c} \cdot N_f = \frac{1}{2}W'_f(2N_f)^{b+c+1} \quad (2-12)$$

We may plot Equation (2-12) on a $\log W - \log (2N_f)$ diagram as shown in Figure 17, where $b + c + 1$ is the slope of the line, and $\frac{1}{2}W'_f$ represents the intercept at one reversal. From Figure 17, we see that the total plastic energy increases as the reversals $(2N_f)$ to cause the specimen failure increases.

CHAPTER III

SPECIMEN AND EQUIPMENT DESIGN

Specimen Design

The general requirements of specimen design utilized in the low cycle fatigue test were as follows.

(1) The reduced cross section must be limited

The maximum load amplitude on the Instron machine is $\pm 5,000$ lb. The metal tested was 1018 cold worked steel having an ultimate tensile strength of about 80,000 psi. Therefore, the reduced cross section could not exceed $\frac{5,000}{80,000} = 0.0625$ in.

(2) The length of reduced portion

Both the extension and contraction of the uniform reduced section of the specimen was measured. The extensometer, Instron model G-51-12, was used for the measurement. The gage length of the extensometer was one inch. The specimen clasper of the extensometer is one-quarter inch in diameter. Therefore, the least total length of the reduced portion of the specimen had to be one and a quarter inches.

(3) The total effective length of the specimen

The total effective length of the specimen must be limited in order to avoid bending buckling; buckling is calculated according to the Euler column equation (7),

$$P_{cr} = K\pi^2 \frac{EI}{l^2} \quad (3-1)$$

$K = \text{a constant}$

$K = 4$ (for fixed-fixed end condition)

$K = 2.046$ (for fixed-pinned end condition)

The effective length was taken to be 3 inches for fixed-fixed end conditions and 3.5" for fixed-pinned end conditions.

(4) Inelastic Buckling

In low cycle fatigue tests, the specimen is always strained into the plastic region (8); therefore, another relation involving inelastic buckling strain must be considered (9):

$$\epsilon_{cr} = \frac{E_t \pi^2}{E_s (Kl/r)^2} \quad (3-2)$$

Examining Equation (3-2), E_t and E_s are the properties of the test material, π and K are constant, and the value of l is fixed. If we desire ϵ_{cr} to have a large value, we must make r , the radius of gyration, large. Thus, a tubular shaped specimen is adopted; the radius of gyration of a tubular specimen is expressed as follows:

$$r = \frac{\sqrt{d_o^2 + d_i^2}}{4} \quad (3-3)$$

(5) Waved buckling

For a constant cross-sectional area, the tubular specimen has a large value of the radius of gyration. Thus, it has a good stability. But, if the thickness of the wall is too small, waved buckling will occur in the specimen. The equation relating to wave buckling (10) should be taken into consideration.

$$P'_{cr} = 3.8 E t^2 \quad (3-4)$$

Equation (3-4) is derived from a theoretical analysis, but tests indicate that the actual critical load should be reduced to forty percent of theoretical waved buckling load, P'_{cr} .

(6) The specimen alignment and dimensions

When the specimen is gripped by the fixture equipment, the specimen should remain in self-alignment. The upper surface of the shoulder should be finished since it will completely contact the upper grip when it is tested. An hour-glass shaped specimen was designed as shown in Figure 18, with the length of the uniform reduced portion, one and a quarter inches. The all-over length is 4 7/8". The tube is 0.312" in inner diameter and 0.375" ± 0.0005" in outside diameter. The specimen has both ends threaded. The upper end is threaded into the upper grip and the other end threaded into a ball or a cylindrical grip, depending on which equipment is used.

(7) Calculation

The area of the uniform reduced section, $A = 0.033 \text{ in}^2$, and the radius of gyration, $r = 0.12195 \text{ in}$. Checking the bending buckling load of Euler column equation, we only need to calculate the critical buckling load of fixed-pinned end condition:

$$P_{cr} = K\pi^2 \frac{EAy^2}{l^2} = (2.046)(3.1416)^2 \frac{30 \times (10)^2 \cdot 0.033 \cdot (0.12195)^2}{(3.5)^2}$$

$$= 40,000 \text{ lb}$$

This critical elastic buckling load is greater than the applied load of 5,000 lb. Waved buckling is then checked,

$$P'_{cr} = 3.8 E t^{2.4} 40\%$$

$$= 3.8 (30) 10^6 (0.0315)^{2.4} = 45,000 \text{ lb}$$

The critical waved buckling load estimated appears to be considerably larger than 5,000 lb.

We evaluate the inelastic buckling strain from Equation (3-2),

$$\epsilon_{cr} = \frac{E_t}{E_s} \frac{\pi^2}{\left(\frac{Kl}{Y}\right)^2}$$

From the monotonic stress-strain curve, we may estimate E_t and E_s by trial. For fixed-fixed end conditions, the critical inelastic buckling strain was evaluated as follows:

$$E_t = 0.40625 \text{ psi} \quad E_s = 4.9 \text{ psi}$$

$$\epsilon_{cr} = \frac{0.40625}{4.9} \frac{\pi^2}{\left(\frac{0.5(3)}{0.12195}\right)^2} = 0.0054 \text{ in/in}$$

For fixed-pinned end conditions,

$$E_t = 0.838 \text{ psi} \quad E_s = 6.714 \text{ psi}$$

$$\epsilon_{cr} = \frac{0.838}{6.714} \frac{(3.1416)^2}{\left(\frac{0.7(3.5)}{0.12195}\right)^2} = 0.00305 \text{ in/in}$$

The critical inelastic buckling strain is calculated according to the theoretical analysis of tangent modulus theory (9), but the actual inelastic buckling is high up to 0.02 in/in for fixed-fixed end conditions and 0.01 in/in for fixed-pinned end conditions in the low cycle fatigue tests.

Fixture Equipment Design

The general requirements for fixture equipment are as follows:

(1) The equipment should provide for a vertical self-alignment of the specimen when the specimen and the equipment are put on the Instron machine.

(2) The gripping condition should satisfy the Euler column boundary condition when the equipment grips the specimen.

(3) The equipment should be made of higher strength and harder material than that of low carbon steel, in order to make sure that the teeth of thread in it would not be damaged during repeated tests.

For the purpose of satisfying vertical alignment, the following pieces need to have a smooth and horizontal surface: upper grip, tension collar, cylindrical lower grip, upper and lower seat of the ball grip and cylindrical base. When these pieces are put together, they contact perfectly and horizontally, and the center lines of upper grip and cylindrical and spherical lower grips, as well as that of the specimen should coincide to make sure the vertical alignment is correct. The assembly views of these two different type grips are shown in Figures 19 and 20. It should be stated that the essential difference between the two types are the lower grips. A 5/8" radius sphere is

used for fixed-pinned end grip arrangements and a cylindrical grip for the fixed-fixed cases. Examining the assembly views of these two types, we see that they satisfy the Euler column boundary conditions.

All the detailed drawing of the equipment parts are shown in Figures 21, 22, and 23.

Comparison of Equipment Used for Low Cycle Fatigue Tests

The equipment used for low cycle fatigue tests are divided as follows:

- (1) The pinned-pinned end condition
- (2) The fixed-pinned end condition
- (3) The fixed-fixed end condition

The pinned-pinned end condition equipment permits the two ends of the specimen to rotate about the end fixtures. The upper grip is a universal joint. The lower grip consists of a 5/8" radius sphere, a spherical seat which can be adjusted horizontally on the base surface for the specimen alignment, a tension collar, and a base.

The assembly process for the tests is as follows: the upper grip is hung on the load cell by a pin passing through the holes in the load cell and upper grip. The upper end of the specimen is threaded into the upper grip. The tension collar is placed below the specimen and raised over the specimen while the lower end of the specimen is threaded into the spherical grip. The specimen aligns vertically by gravitation. The base is fastened on the crosshead beam and the spherical seat is put on the base. Move the crosshead up until the surfaces of the 5/8" radius sphere, sphere seat and base have a perfect contact, and then fasten

the tension collar to the base. During the fastening process, the crosshead beam position (up and down) and the sphere seat horizontal position must be adjusted so that the load pen stays on the middle point of the chart (zero load point) in order to make sure that there is no preload in the specimen.

This fixture equipment is weaker in compression than the other two fixture conditions. It does not satisfy the low cycle fatigue test for the high strength materials. Thus, it is not adopted in this experiment. But, it is a suitable fixture for low cycle fatigue tests in the conditions of simple tension, and tension with small compression, because it places a small restriction moment on the end of the specimen.

The fixed-pinned end condition only permits the low end of the specimen to rotate about the lower fixture. The upper grip is a cylinder, both ends of which are threaded and finished with a horizontal plane. The lower grip consists of a tension collar, a 5/8" spherical grip, an upper and lower seat, and a base.

The assembly process for tests is as follows: The upper grip is threaded tightly into the load cell by a tightening pin passing through the hole in the upper grip. The lower end of the specimen is threaded into the 5/8" spherical grip. The upper seat and tension collar are placed over the specimen and put into position on the spherical seat. Then, the lower seat is connected to the upper seat using the four adjusting screws. This process unites the upper seat, spherical grip, and lower seat. The lower base is next fastened to the crosshead of the testing machine. Then, the crosshead is moved up and finally the

tension collar is fastened to the base. Thus, the assembly process is completed as shown in Figure 18. During the assembly process, care is taken to maintain zero load on the specimen; this is accomplished by observing the load indicating pen on the testing machine.

The fixed-fixed end condition fixes both ends of the specimen rigidly. This condition produces the greatest restriction moment on both ends of the specimen, and this considerable restrictive moment will effect the low cycle fatigue data. But, this fixture gives the specimen the best stability. If suitable self-alignment is accomplished, the material may be tested to a large completely reversed strain amplitude.

The fixed-fixed end fixture includes the following parts: upper grip, tension collar, cylindrical grip and base. The assembly process for tests is deivided into the following steps:

- a. Thread the upper grip into the load cell tightly by a tightening pin passing through the hole of the upper grip.
- b. Thread the specimen into the cylindrical lower grip and place the tension collar over the specimen, and put into position on the cylindrical lower grip.
- c. Tightly thread the upper end of the specimen into the upper grip.
- d. Move the crosshead up and fasten the tension collar to the base.

- e. Make sure the surfaces of the base and cylindrical lower grip are in contact.
- f. During the assembly process, the load pen on the testing machine should be maintained on the zero point.

CHAPTER IV

OPERATION, DATA AND RESULTS

Strain Measurement and Control

Operation of the testing machine followed the Instron Instruction Book. The crosshead beam speed used was 0.5 in/min. The load range was $\pm 5,000$ lb., with the indicating pen set on the middle of the chart paper. The chart was set to move ± 10 -inch, corresponding to the extensometer expressing a strain of $\pm 10\%$. The extensometer employed was the Instron Model G-51-12, with one inch gage length and 50% maximum strain. Between the two clamped support knives, there was a one-inch gage length spacer which would deter the compression stroke; therefore, the extensometer had to be modified. Four washers were put between the open section of the cover and the knife edge. Thus, the extensometer could be used in extension and compression. Another one-inch gage length space was made by the author and used instead of the gage length spacer provided with the extensometer.

The automatic cycling capability of the Instron machine does not satisfy these test conditions, because a constant moving range of the crosshead beam does not provide a constant strain level for the testing section of the specimen. Therefore, it was necessary to watch the chart roll for control strain level, and manual operation was used during the tests.

A series of constant range tests which produced fatigue life varying from a few reversals ($2N_f$) to several thousand reversals was

made on 1018 cold worked steel. The specimens were subjected to axial-load completely reversed strain amplitude cycling. Cyclic stress amplitude was measured periodically throughout the tests. From these data, the analysis of fatigue properties were investigated.

Data and Results

Mechanical properties of 1018 cold worked steel:

Ultimate strength, $\sigma_u = 80,000$ psi

True fracture strength, $\sigma_f = 140,000$ psi

True fracture ductility, $\epsilon_f = 0.16$ in/in

TABLE 1

Fatigue Properties of 1018 Cold Worked Steel

n'	ϵ'_f in/in	σ'_f psi	b	c	Transition Life
0.15	0.16	88,500	0.0805	0.537	6800R

TABLE 2

Half Life Cyclic Stress and Plastic Strain
at Several Constant Strain Amplitude Tests

Total Strain Amplitude	0.02	0.015	0.01	0.008	0.006	0.004
Plastic Strain Amplitude	0.01791	0.01317	0.00816	0.00625	0.004323	0.002437
Stress Amplitude	62,500	59,400	55,000	52,500	50,312	46,875

Some fatigue properties of 1018 cold worked steel are plotted in the following figures:

Cyclic stress amplitude-number of reversals at several different strain amplitudes. Figure 10

Plastic strain energy per cycle as a function of strain reversals. Figure 11

Fatigue ductility properties. Figure 13

Fatigue strength properties. Figure 14

Total cyclic strain-life in reversals. Figure 15

Plastic energy per cycle-life in reversals. Figure 16

Total plastic energy-life in reversals. Figure 17

CHAPTER V

CONCLUSIONS AND RECOMMENDATIONS

The principal aims in performing this work were as follows:

- (1) to obtain satisfactory low cycle fatigue data for 1018 cold worked steel;
- (2) to design two types of equipment for gripping the specimen and use both for the tests;
- (3) to follow the plastic hysteresis energy equations derived by JoDean Morrow, and used to develop an understanding of low cycle fatigue properties of 1018 cold worked steel.

Four fatigue properties, ϵ_f' , σ_f' , C, and b, are very important for the calculation of plastic strain energy. σ_f' is related to the true fracture strength, and ϵ_f' to the true fracture ductility. So far, there are no adequate relationships established between ϵ_f and ϵ_f' , and σ_f' and σ_f . It is only known that σ_f' is close to σ_f , and ϵ_f' close to ϵ_f .

During the completely reversed cyclic tests in strain, it was observed that for 1018 cold worked steel the fatigue strength coefficient σ_f' was much smaller than the true fracture strength σ_f . This is because, in constant strain cyclic tests, softening occurs in 1018 cold worked steel. The half life cyclic stress is always smaller than the initial stress. If the tested material were changed to another material which has a cyclic hardening behavior, the half life cyclic stress would be larger than the initial stress and the fatigue strength coefficient would be close to the true fracture strength.

The fatigue strength relation is similar to Basquin's equation. Basquin conducted his experiment in a constant load condition. The author tested in constant strain condition in order to calculate the plastic strain energy from the hysteresis loop of constant strain range.

The two types of equipment are both suitable for fatigue testing. The fixed-fixed end type is good for use in large strain amplitude tests up to 0.02 in/in without wavy and bending buckling. The fixed-pinned end equipment should be used in small strain amplitude not exceeding 0.01 in/in and produces better results than that of the fixed-fixed end equipment.

The author would like to recommend the following:

(A) The specimen should be improved

The shoulder of the glass-hour shaped specimen has a good contact with upper grip. The lower end should also be shaped as the upper end; thus, the whole specimen can be gripped in a good condition of stability.

(B) The use of automatic control

A brief circuit of automatic control system is sketched as shown in Figure 24.

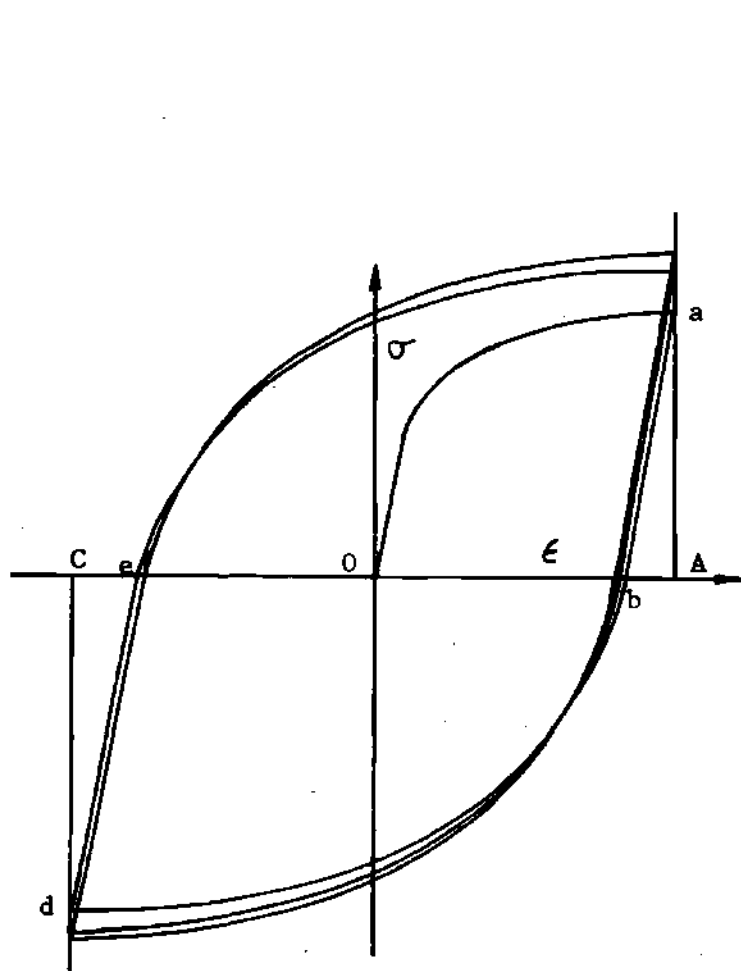
(1) The input terminal is plugged into the strain gage pre-amplifier on the Instron machine.

(2) Input signal is amplified by multi-amplify stages until the output voltage reaches a suitable value.

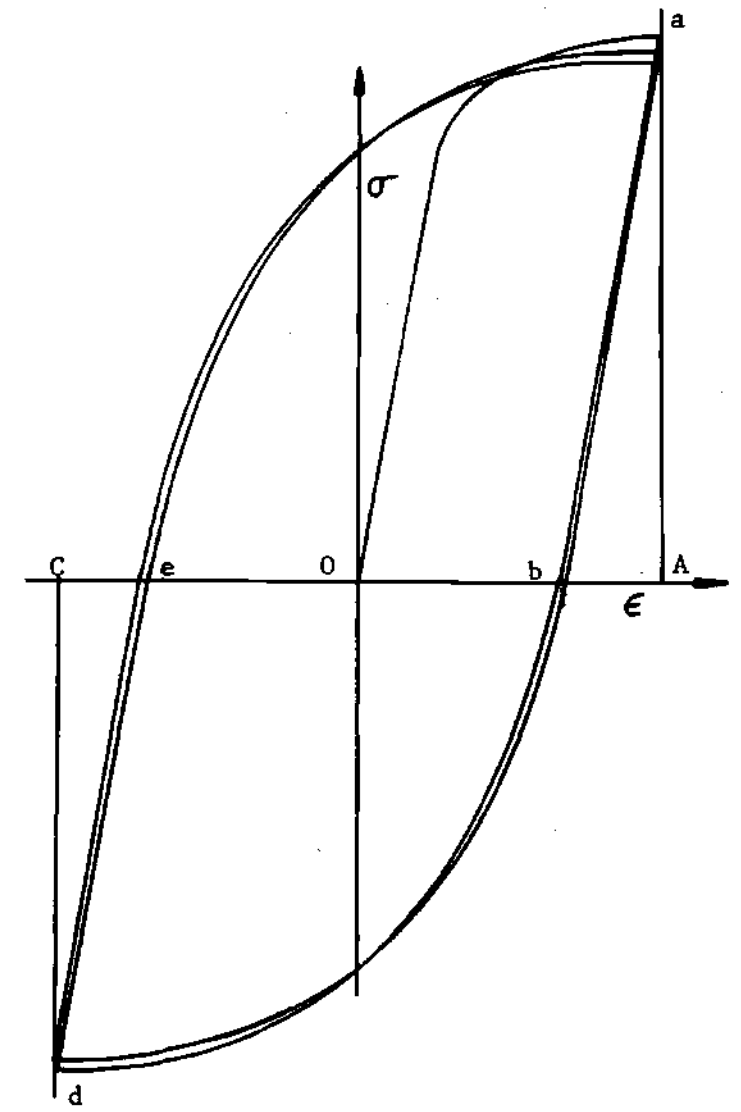
(3) Use a precise reference voltage source in the relay system to control the cross head motion in order to get a

constant strain change of the reduced portion on the specimen which the extensometer measures.

(4) The relay system is connected directly to the driving motor system of the Instron machine. It will control the motion of the crosshead beam.



(A) Cyclic Hardening



(B) Cyclic Softening

Fig. 1 Illustration of Cyclic Hardening and Cyclic Softening

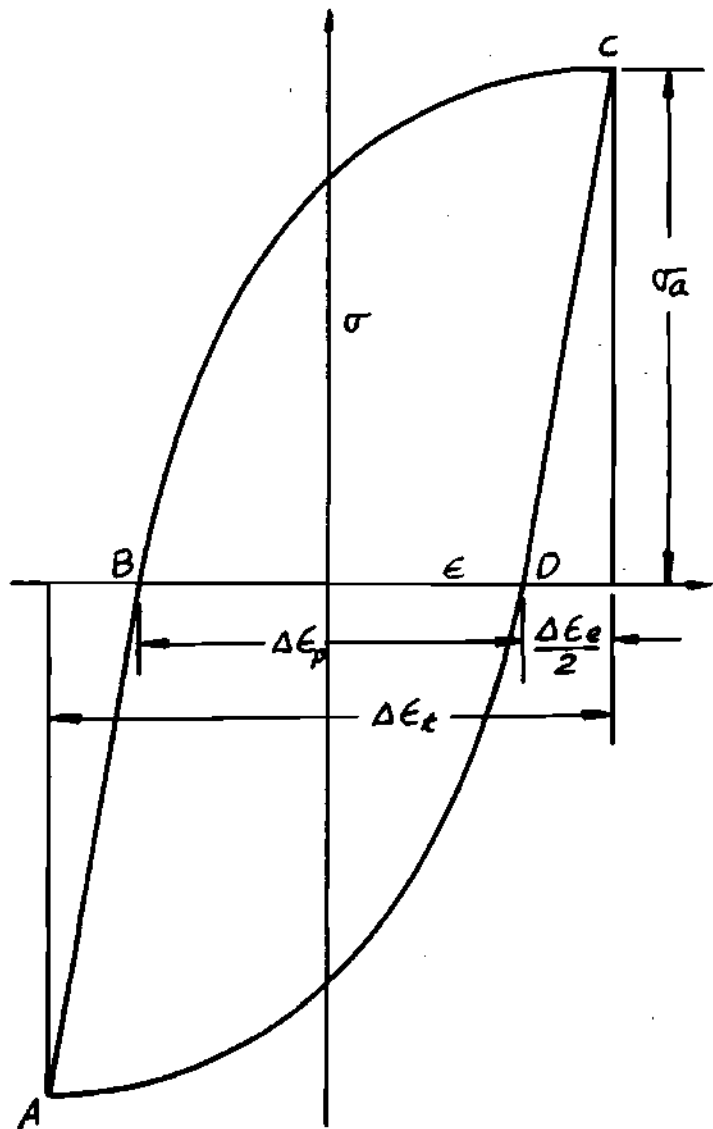


Fig. 2 Hysteresis Loop at Stable Condition.

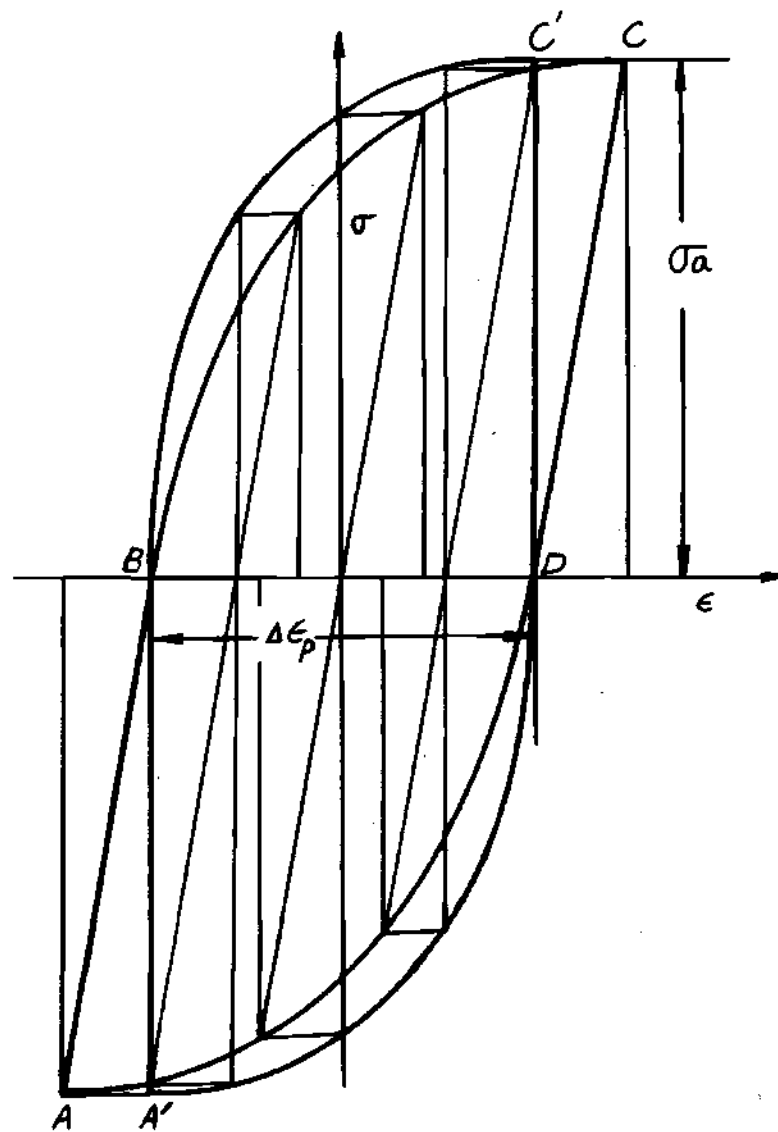


Fig. 3 Hysteresis Loop Converted to Stress-plastic Strain Relation from Stress-strain Plot.

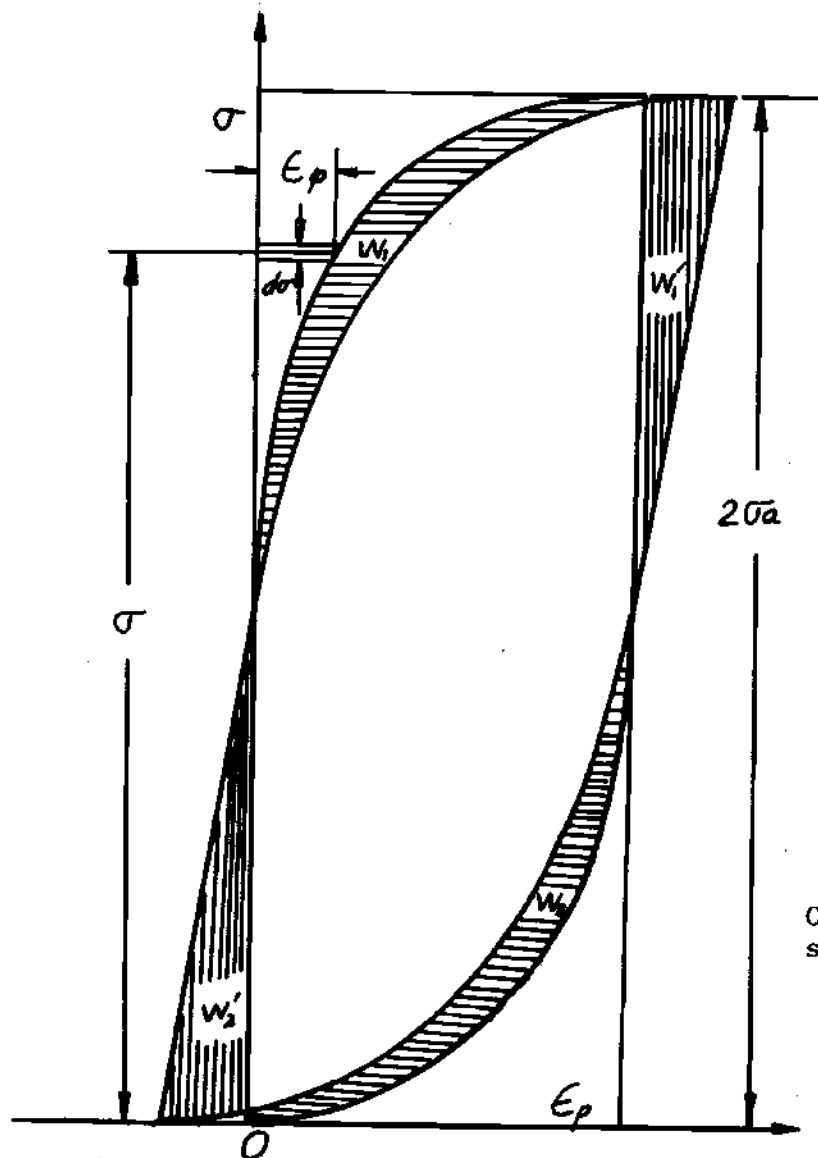


Fig. 4 Illustration of Plastic Energy Calculation.

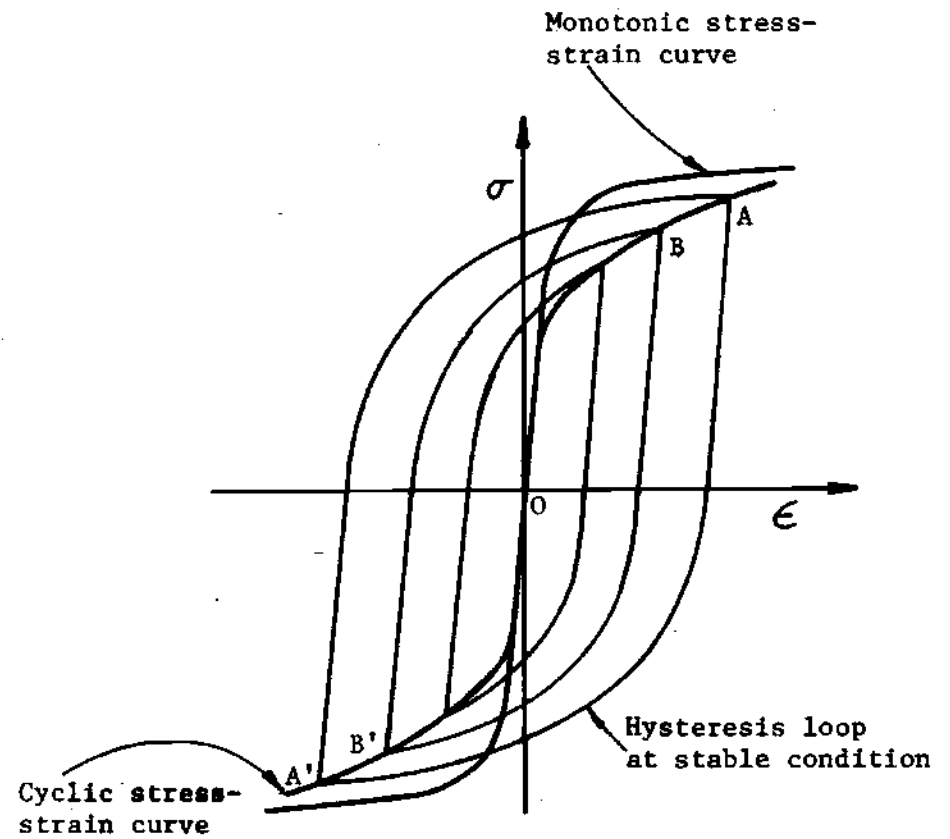


Fig. 5 Illustration of Cyclic Stress-Strain Curve Established by Multiple Step Tests.

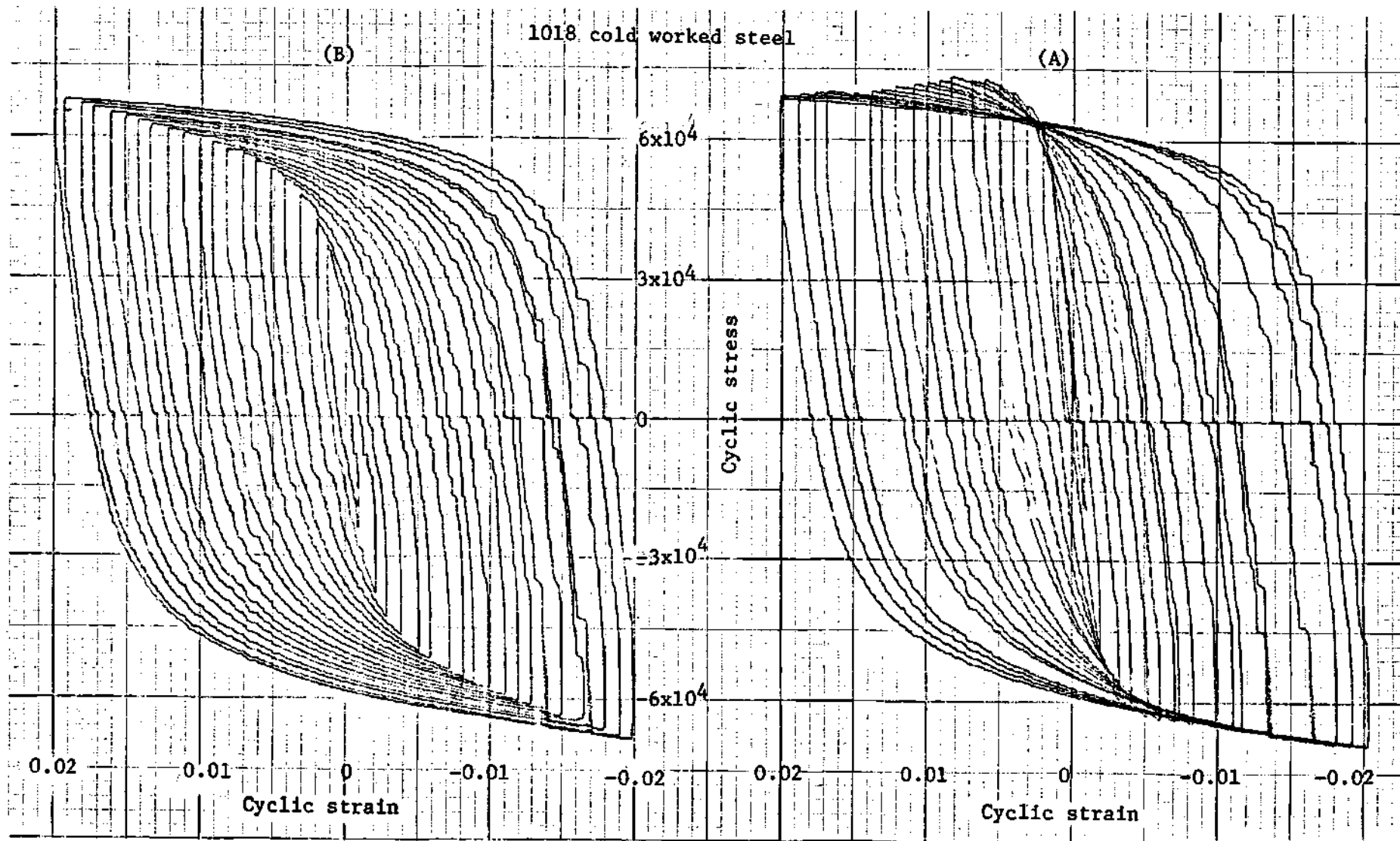


Fig. 6. Cyclic Stress-Strain Curve Established By Incremental Step Tests.

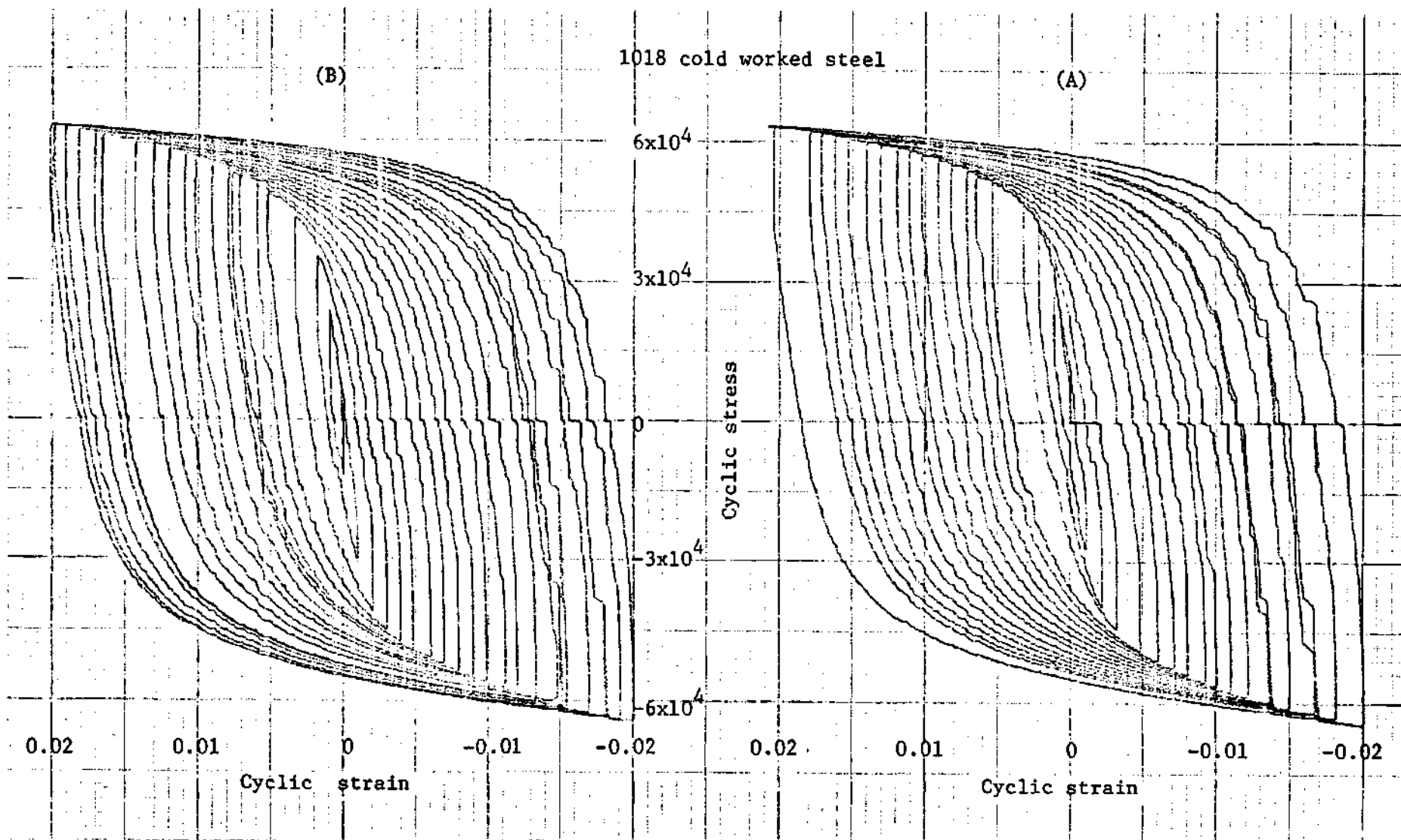


Fig. 7 Cyclic Stress-Strain Curve Established By Incremental Step Tests.

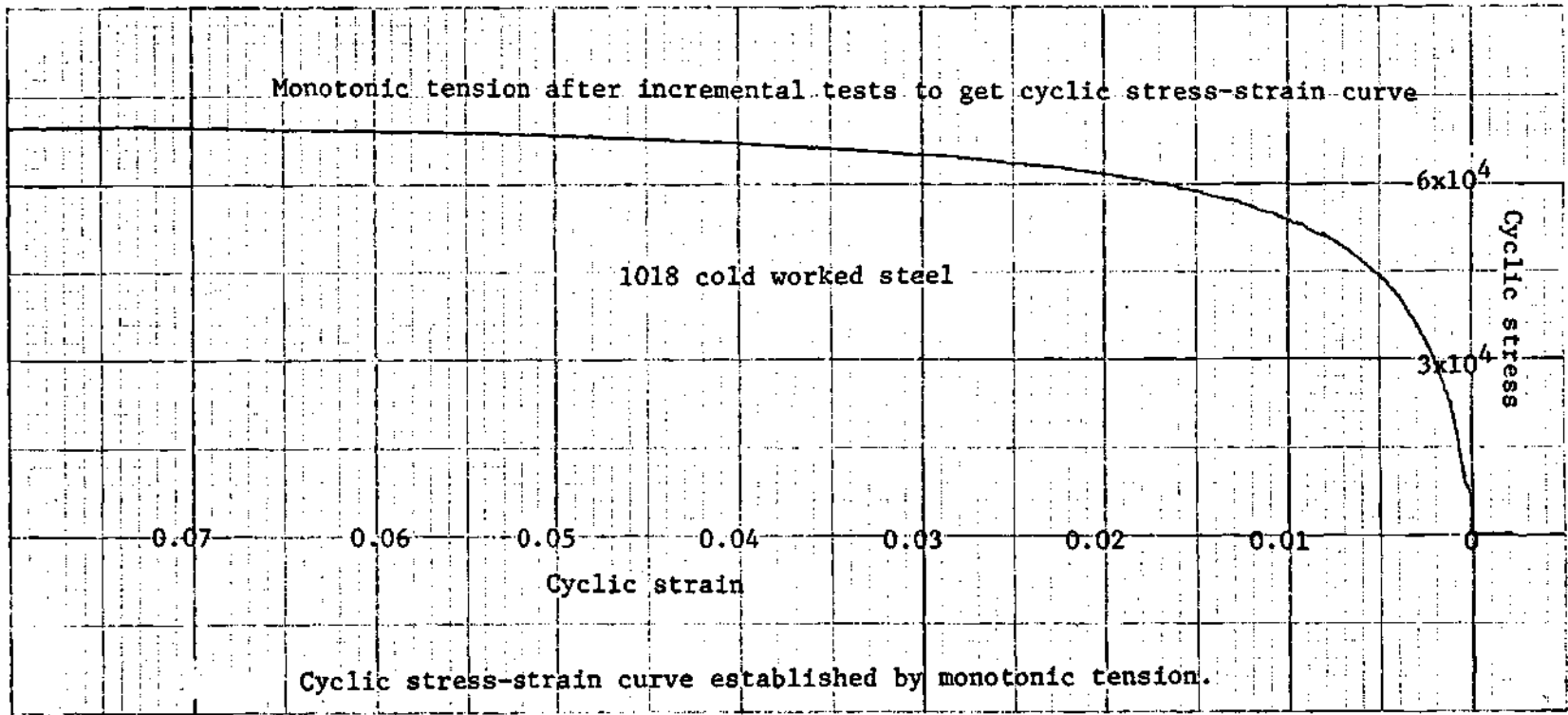


Fig. 8 Cyclic Stress-Strain Curve Established By Monotonic Tension.

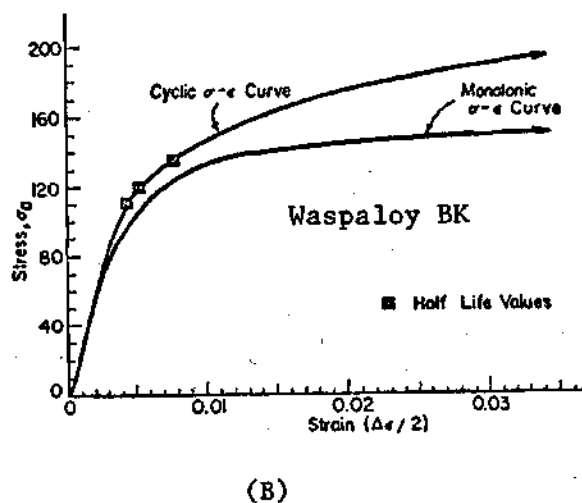
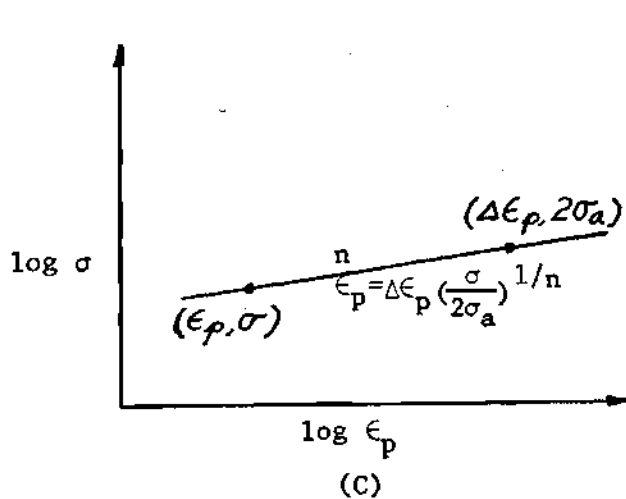
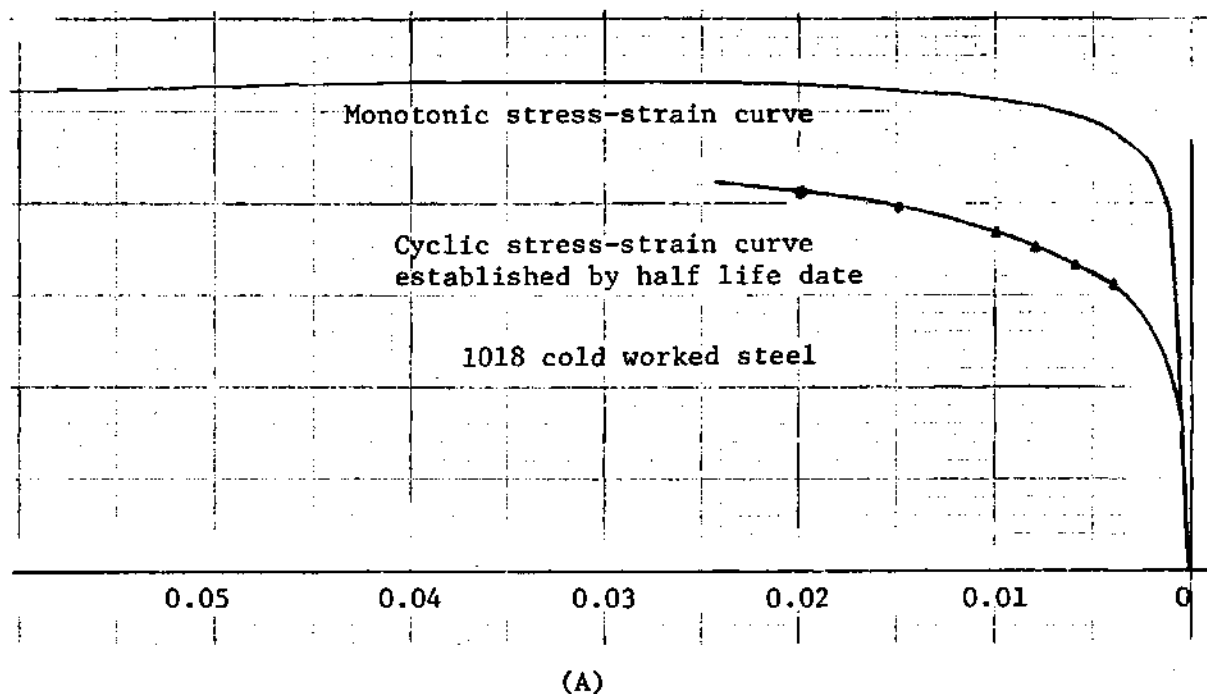


Fig. 9 (A) Comparison of Monotonic Stress-Strain Curve and Cyclic Stress-Strain Curve (Cyclic Softening Material).
 (B) Comparison of Monotonic Stress-Strain Curve and Cyclic Stress-Strain Curve (Cyclic Hardening Material).
 (C) Illustration of Plastic Strain Hysteresis Loop on the log-log Scale.

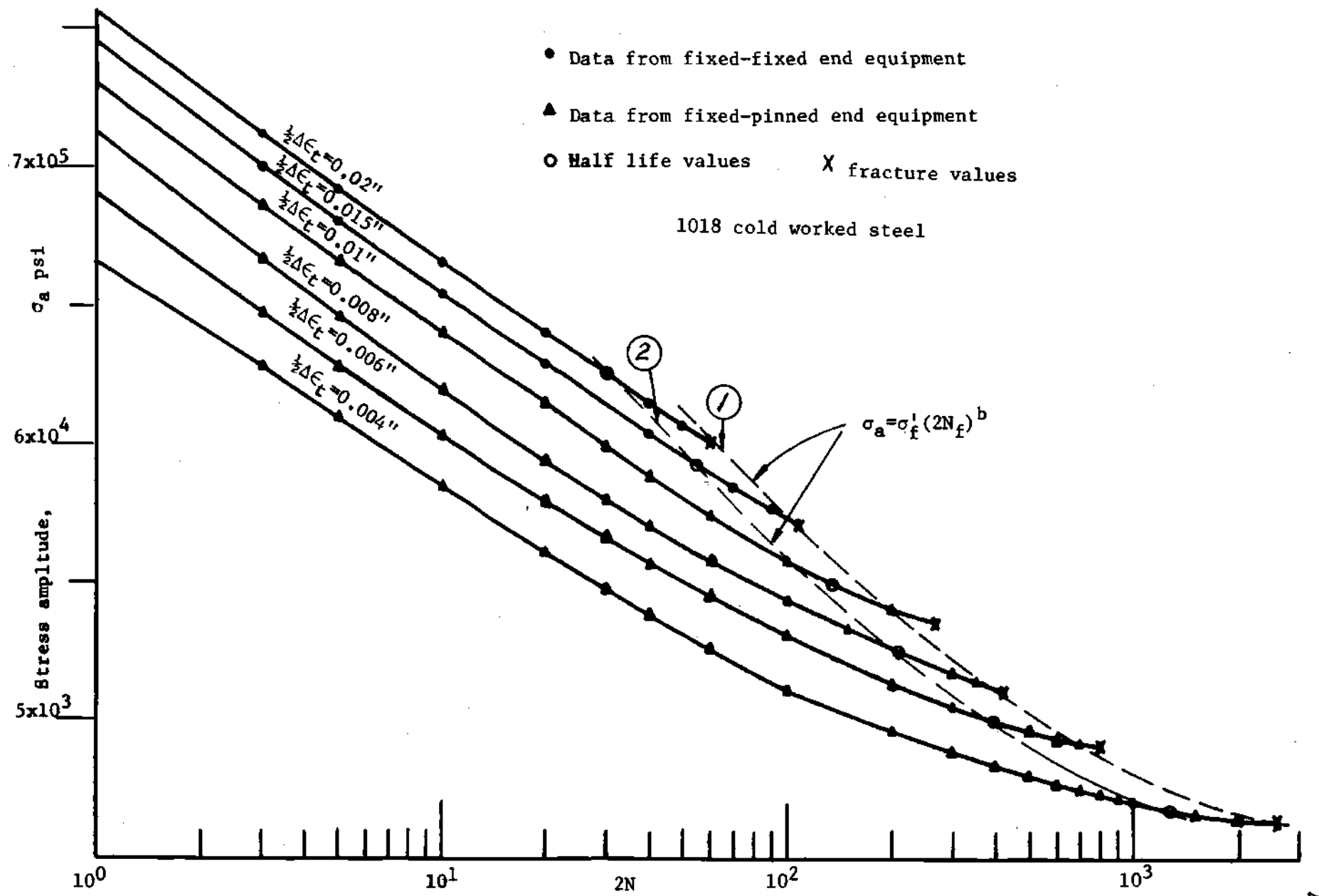


Fig. 10 σ_a - $2N$ Curve of Cold Worked Steel.

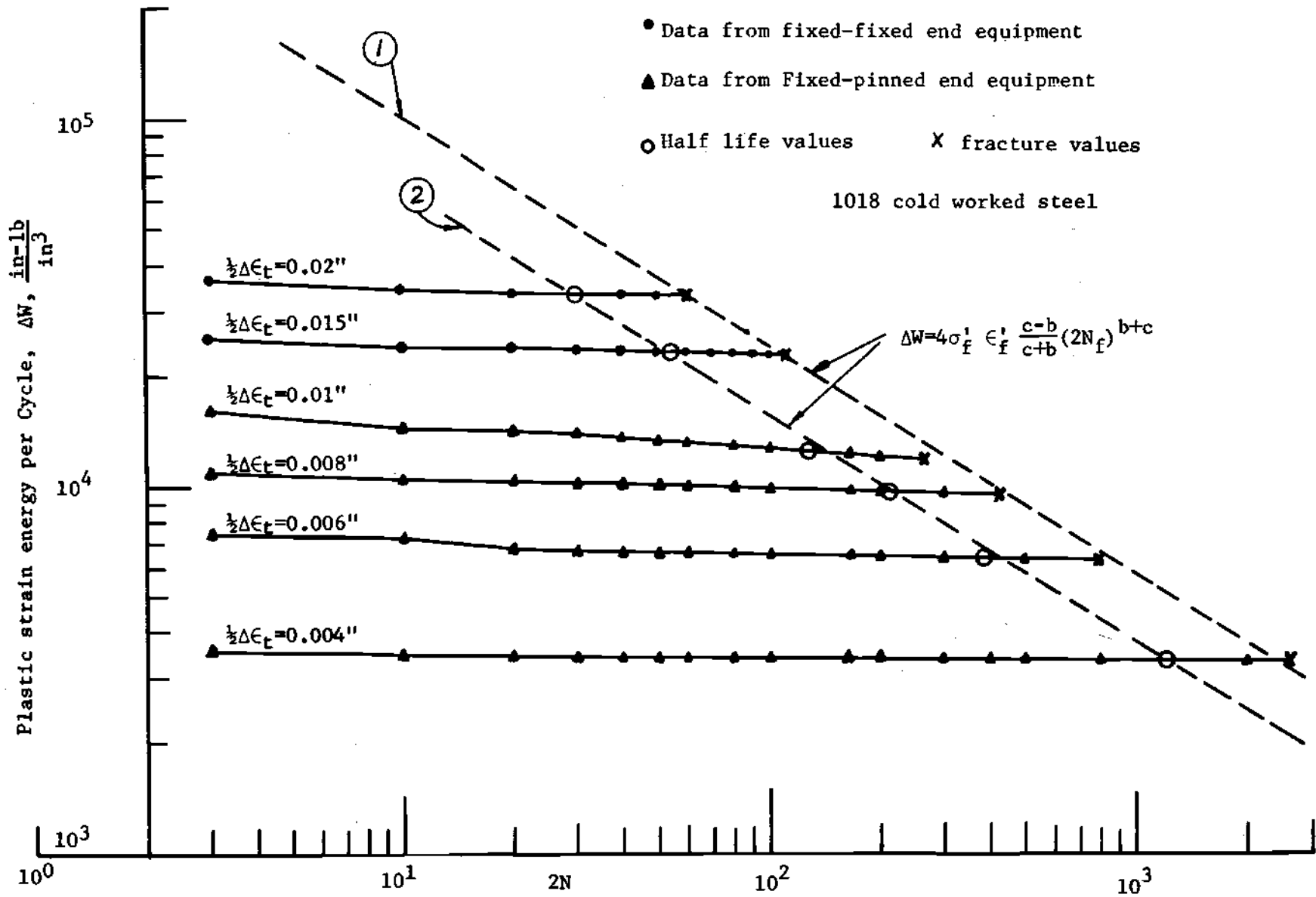


Fig. 11 Plastic Strain Energy As a Function of Number of Reversals.

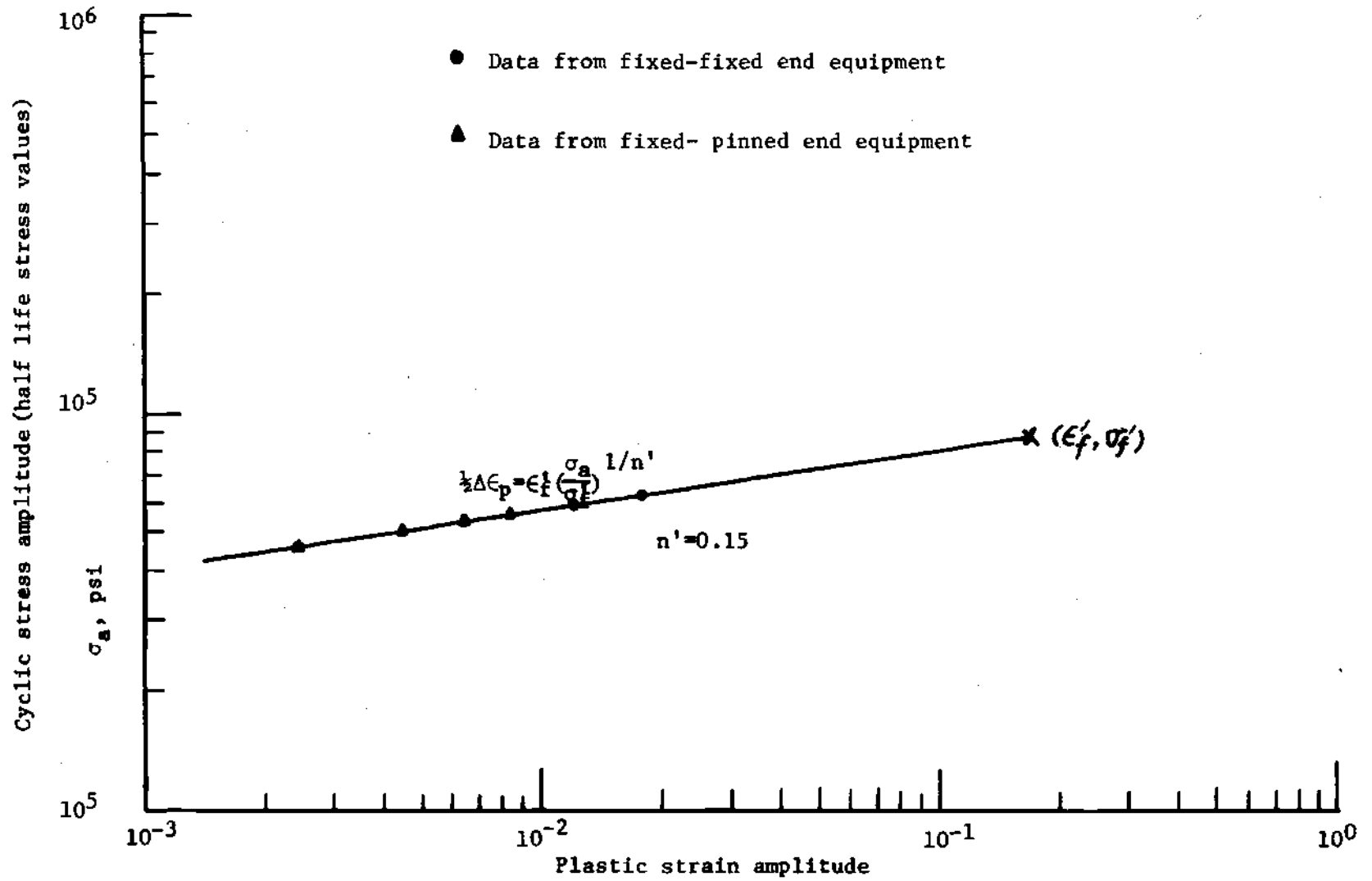


Fig. 12 Cyclic Stress-Plastic Strain Line on a log-log Scale.

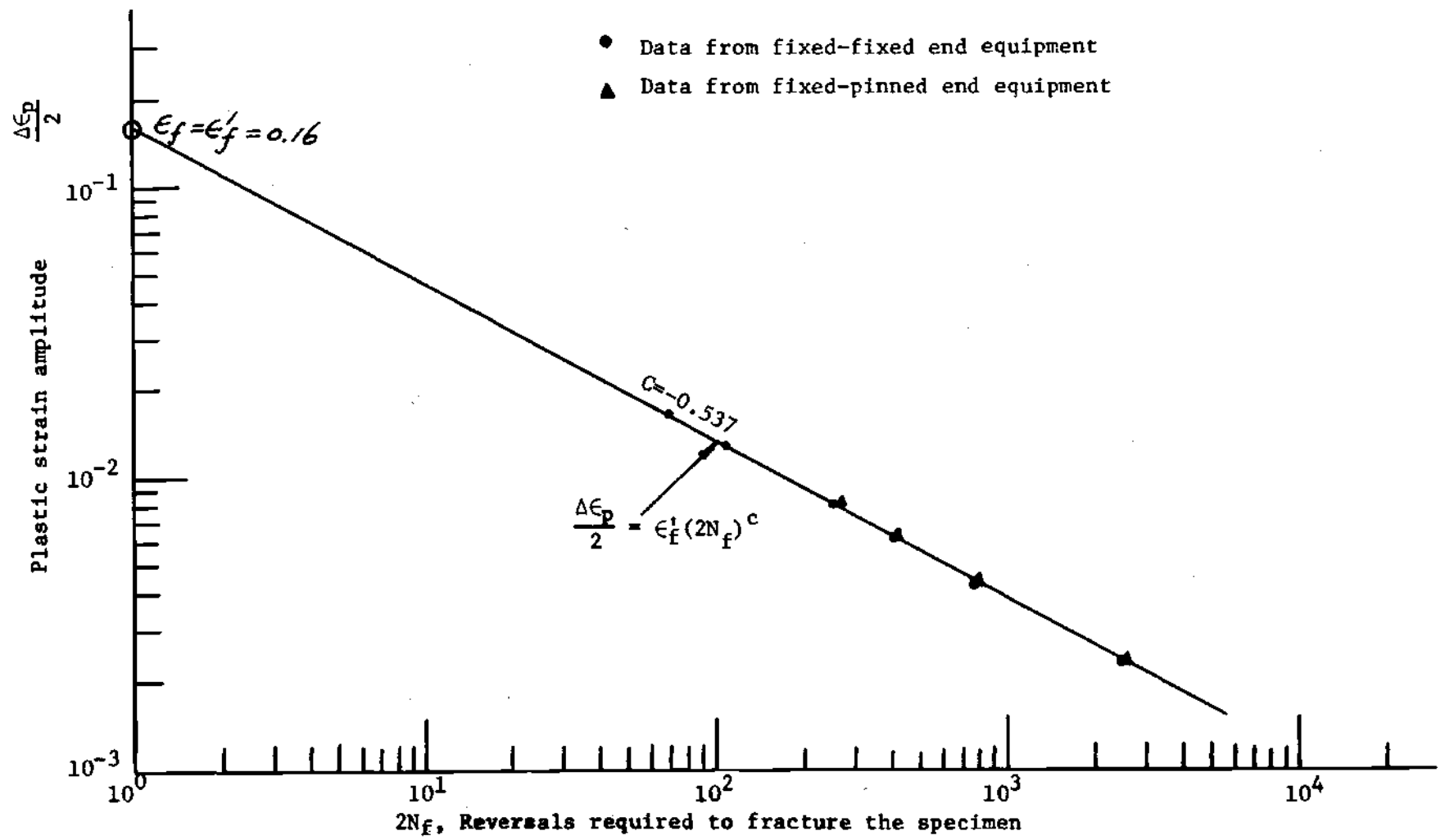


Fig. 13 Fatigue Ductility Properties.

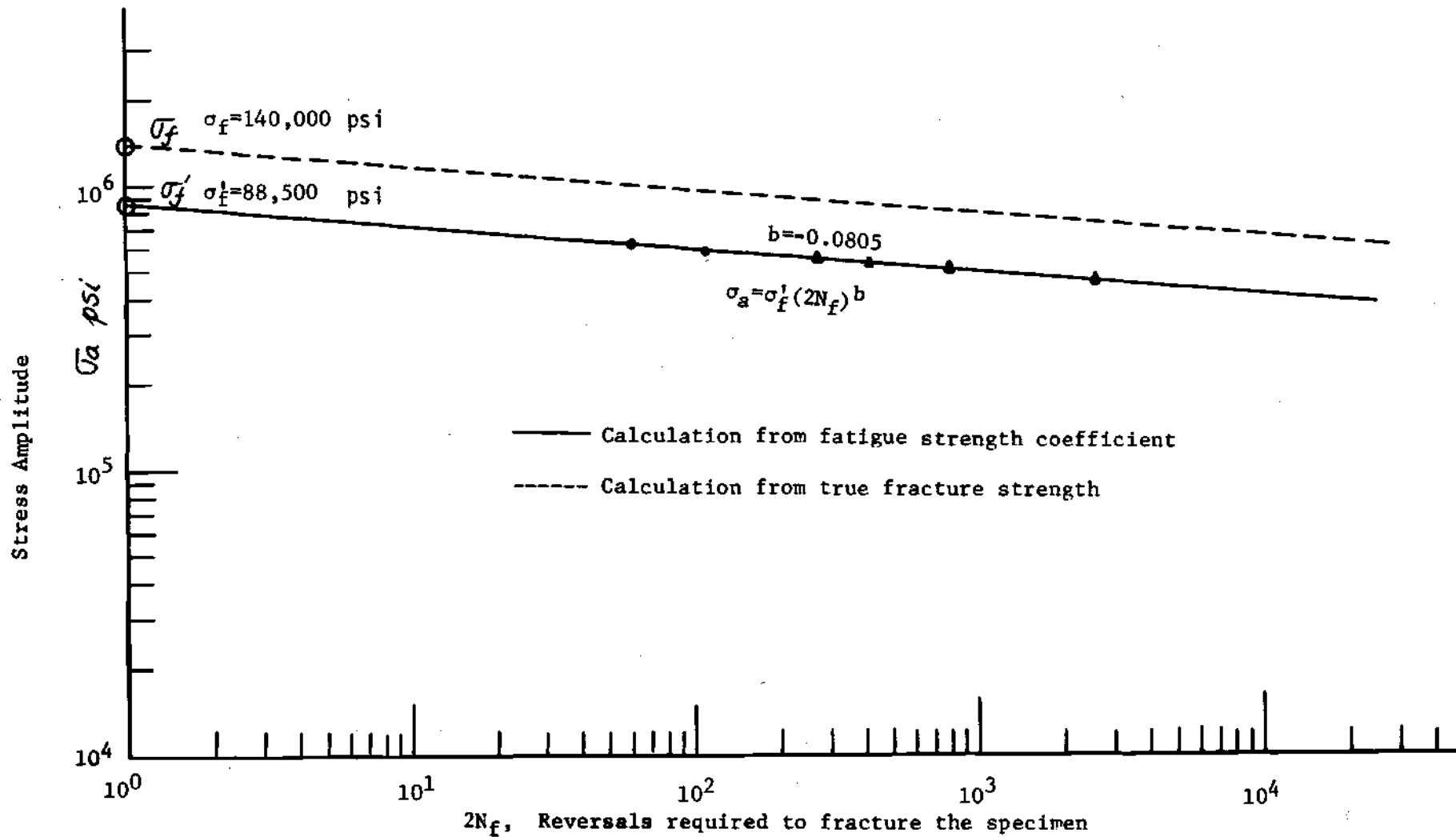


Fig. 14 Fatigue Strength Properties.

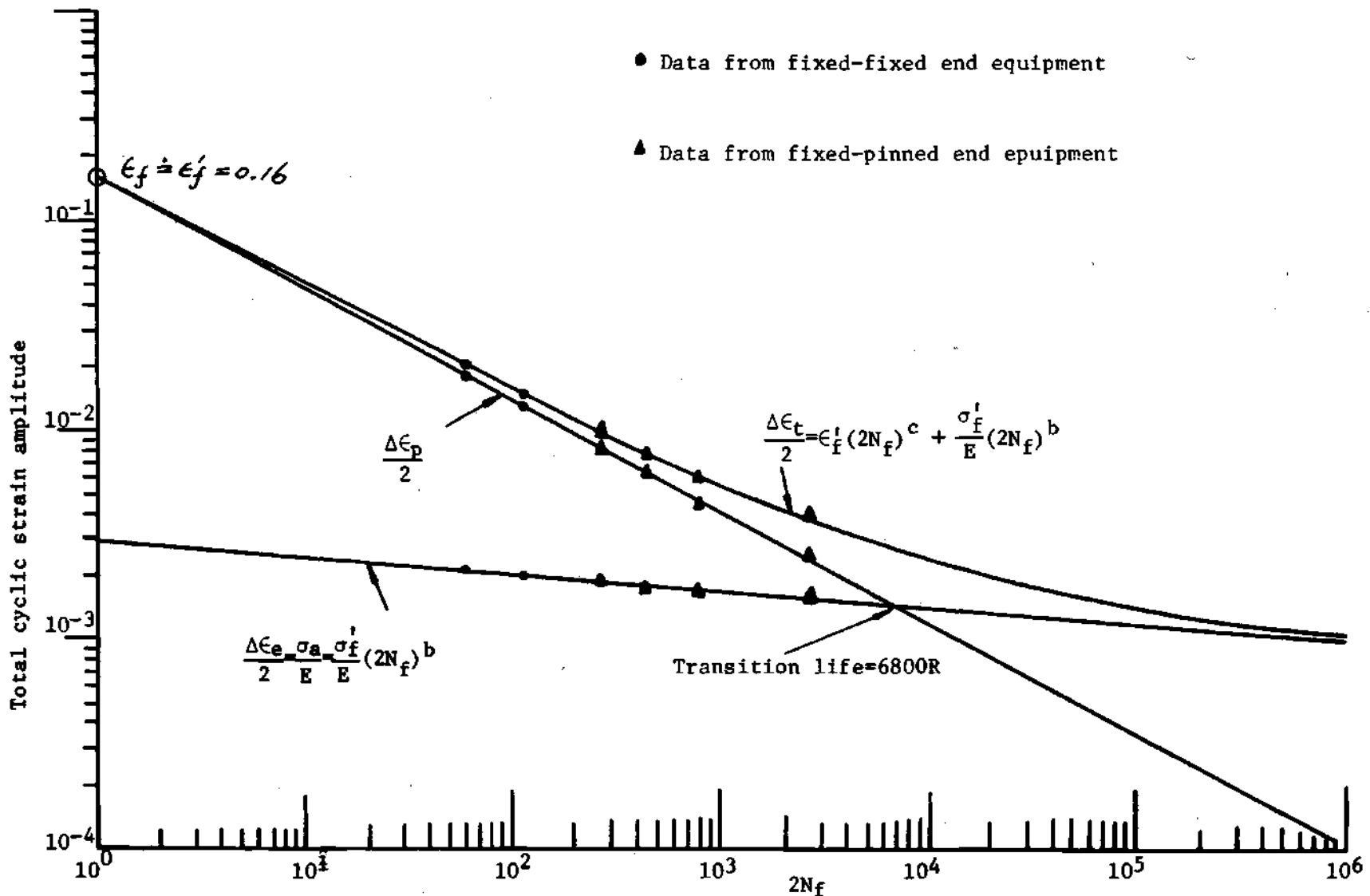


Fig. 15 Total Cyclic Strain-Life in Reversal.

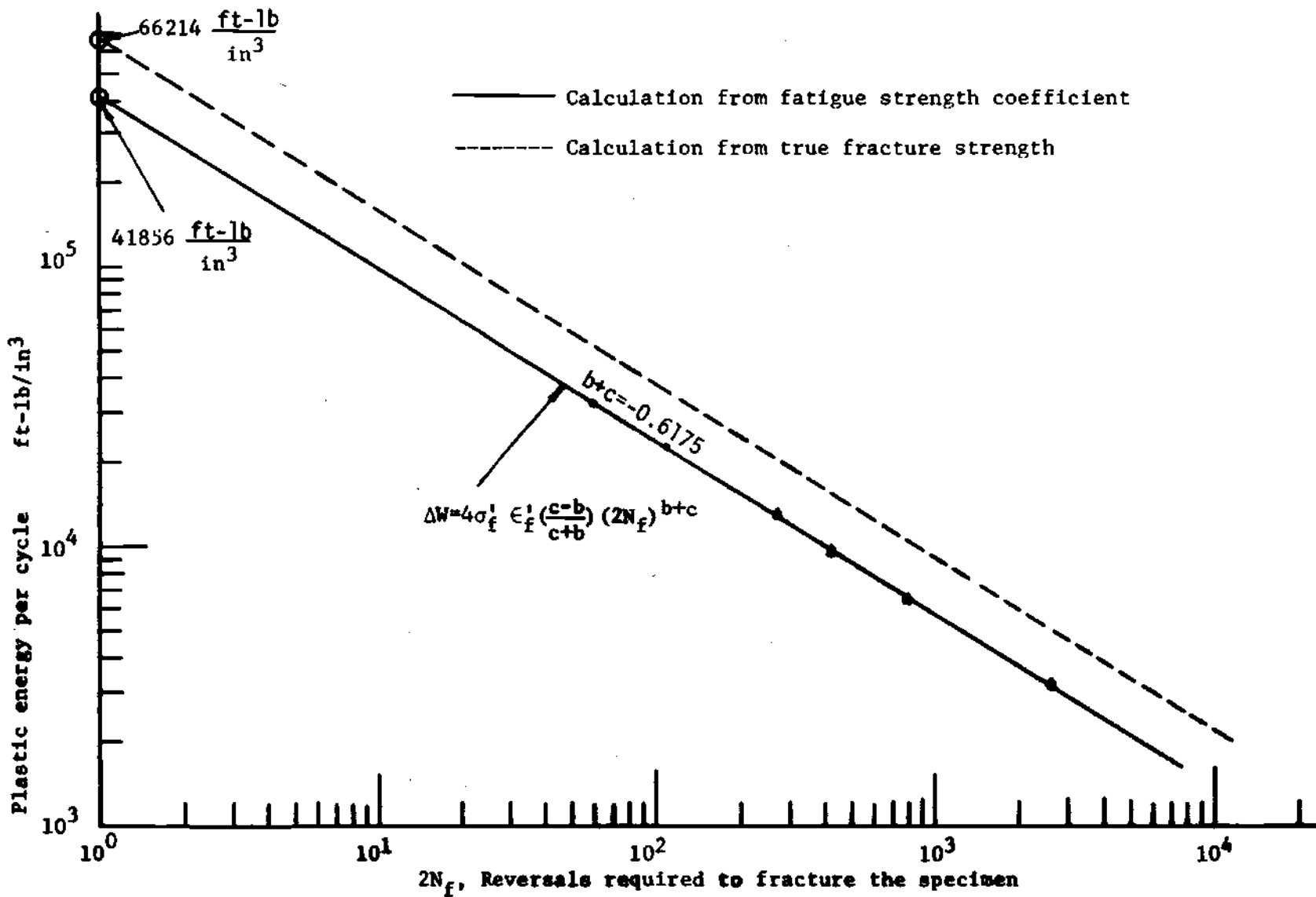


Fig. 16 Plastic Energy Per Cycle-Life in Reversals.

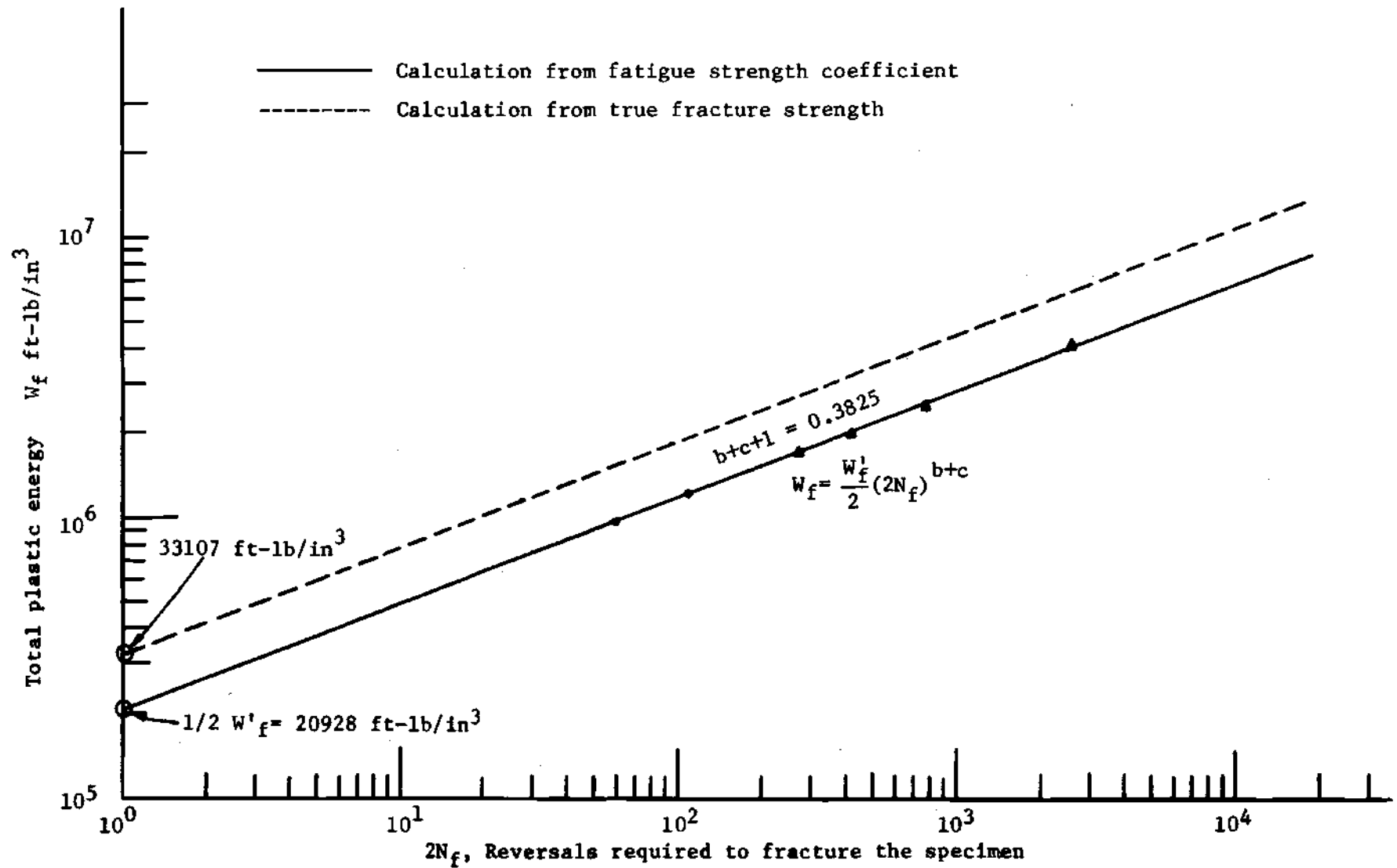


Fig. 17 Total Plastic Energy-Life in Reversals.

Reversed-axial-load specimen

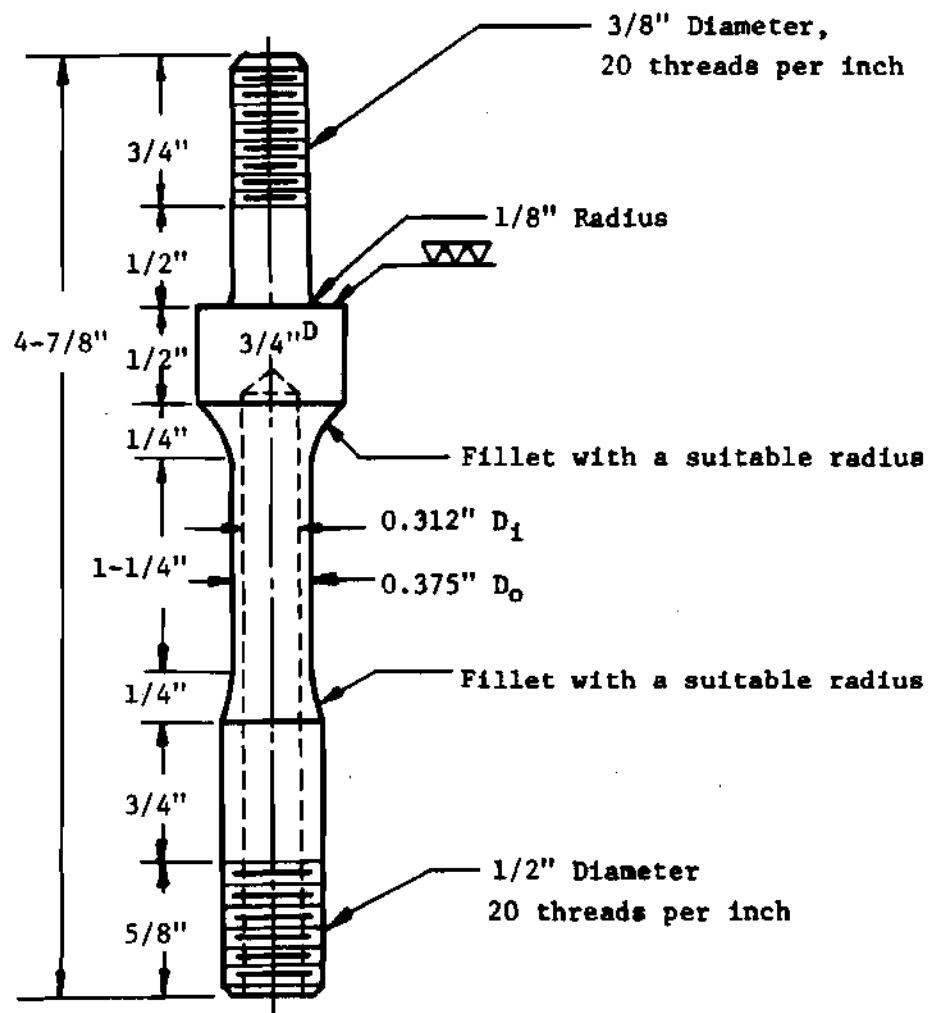


Fig. 18 Specimen Dimensions

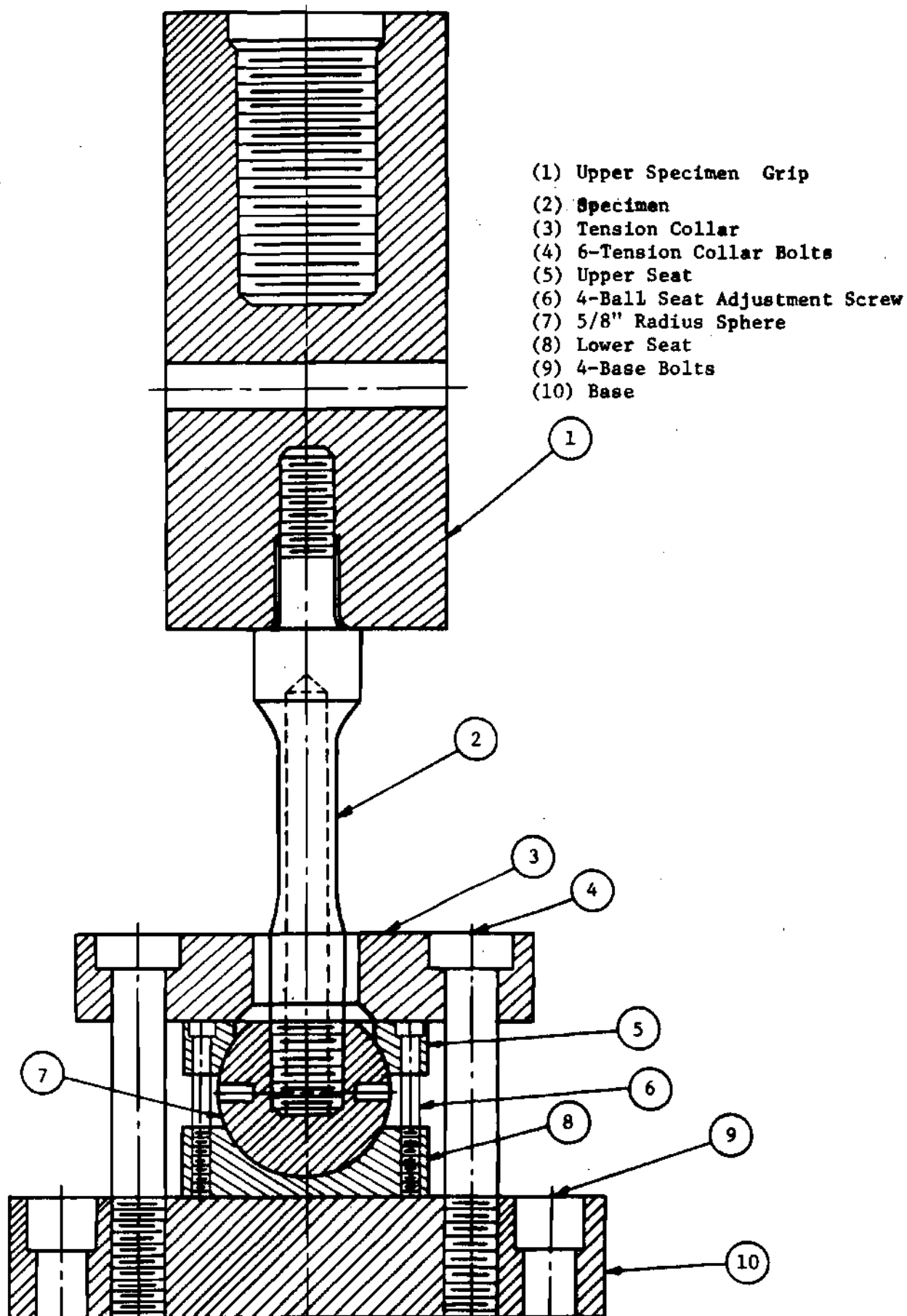


Fig. 19 Assembly View of Reversed-Axial-Load Test Equipment (Fixed-Pinned End).

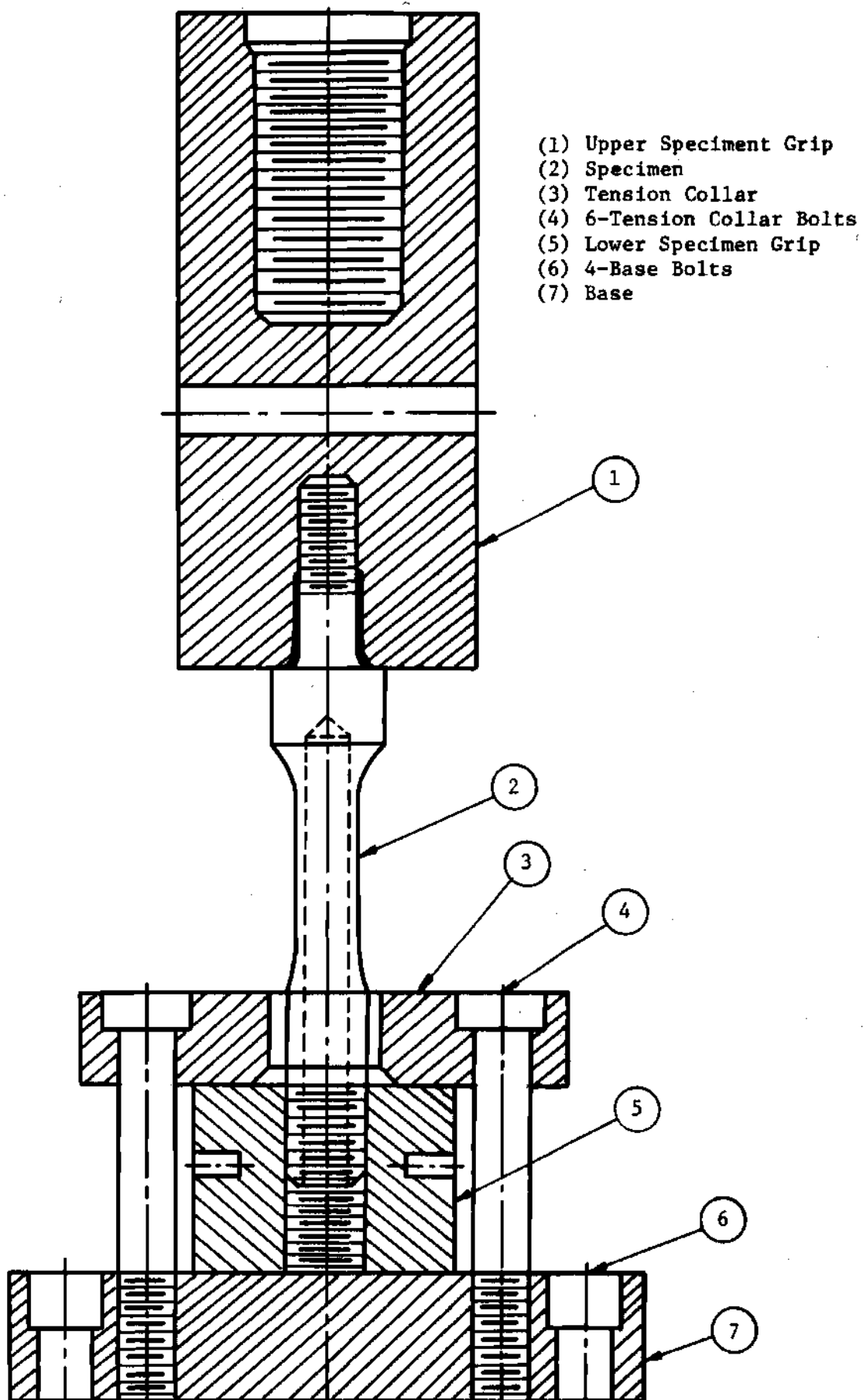
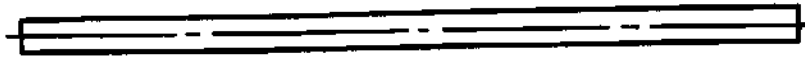


Fig. 20 Assembly View of Reversed-Axial- Load Test Equipment (Fixed-Fixed End).

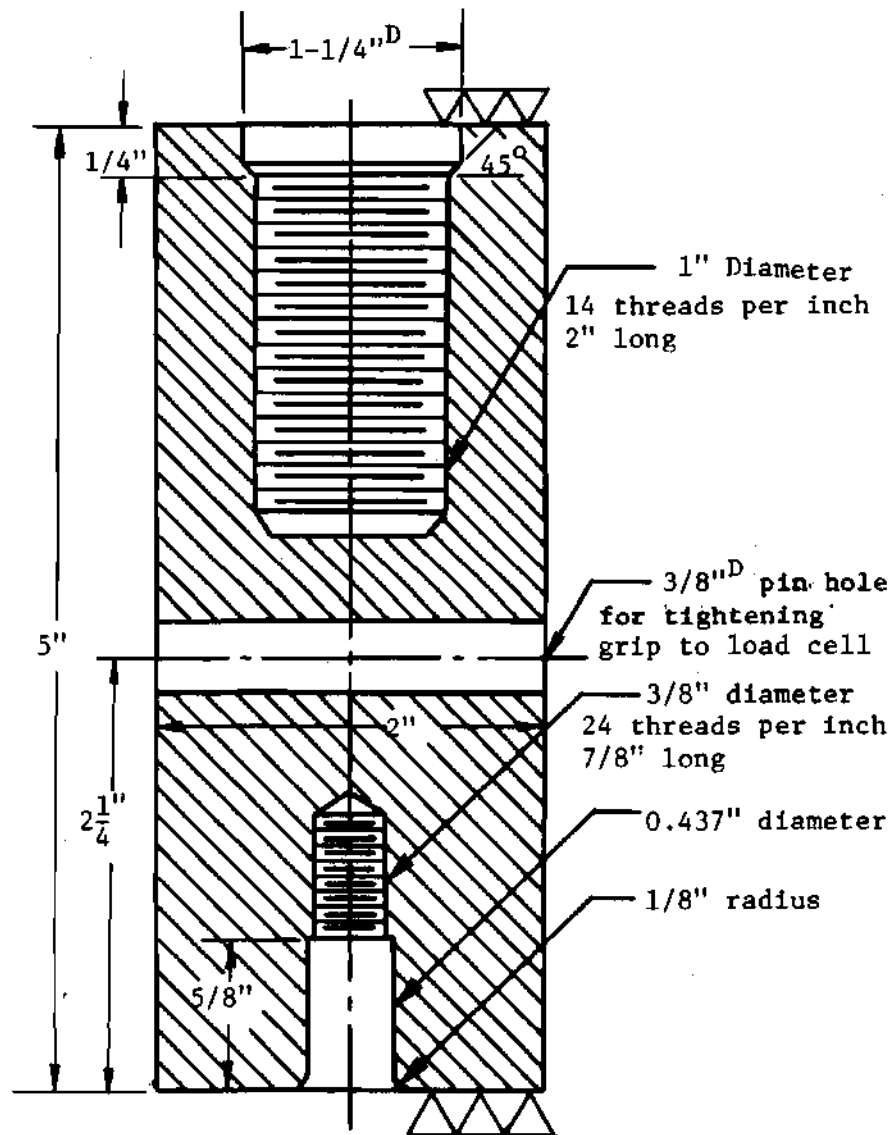
Upper Grip Tightening Pin

8" long, 5/16" diameter.

Scale: Half size



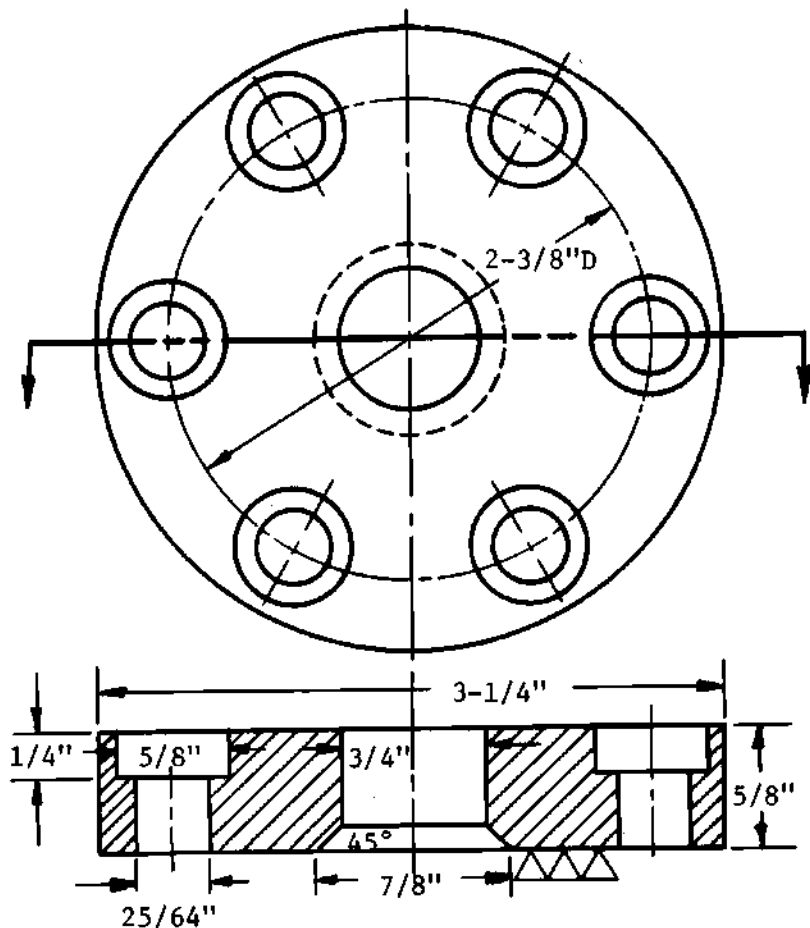
Upper Specimen Grip



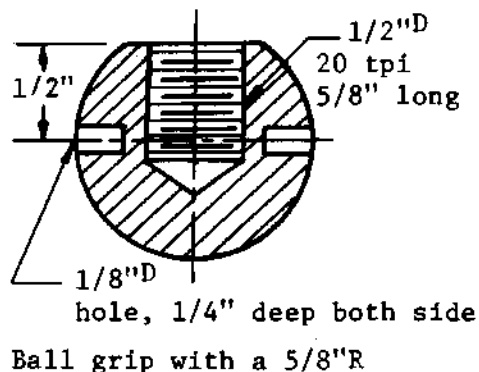
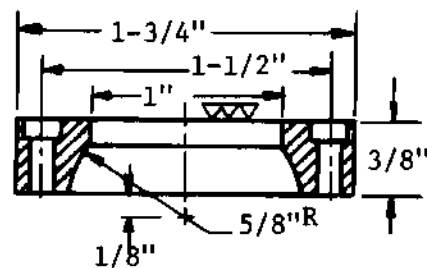
Scale: Full size

Fig. 21 Dimensions of Equipment Parts.

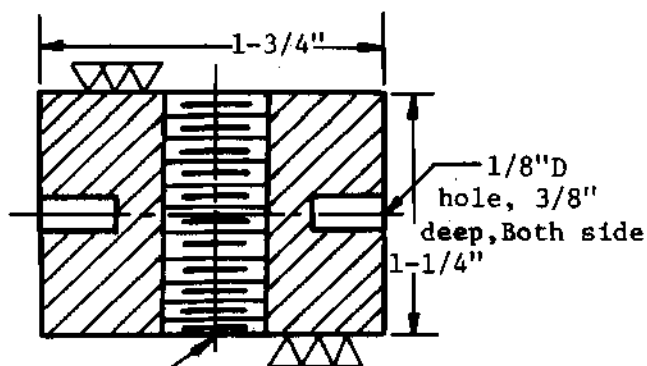
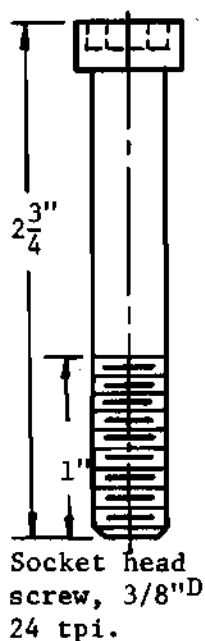
Tension Collar



Upper Seat



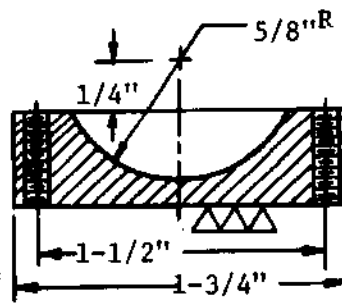
Tension Collar Bolt



1/2" D, 20 tpi
Spherical Lower Grip

Sphere Tightening Pin
2-pin, 2" long, 7/64" D

Lower Seat



Sphere seat adjustment screw

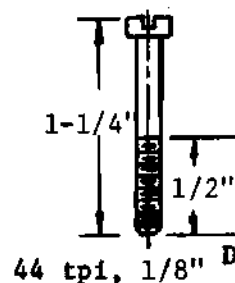


Fig. 22 Dimensions of Equipment Parts.

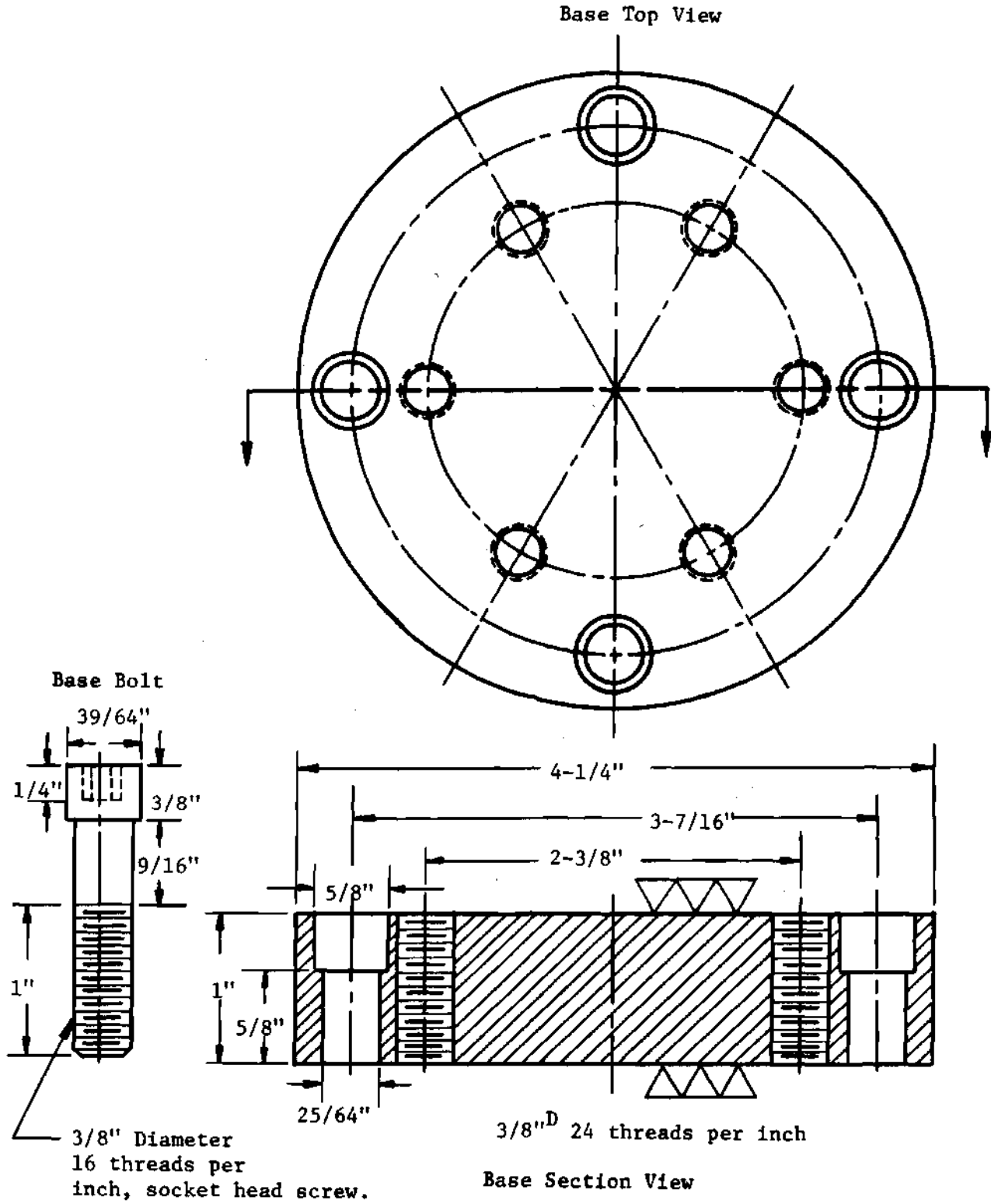


Fig. 23 Dimensions of Equipment Parts.

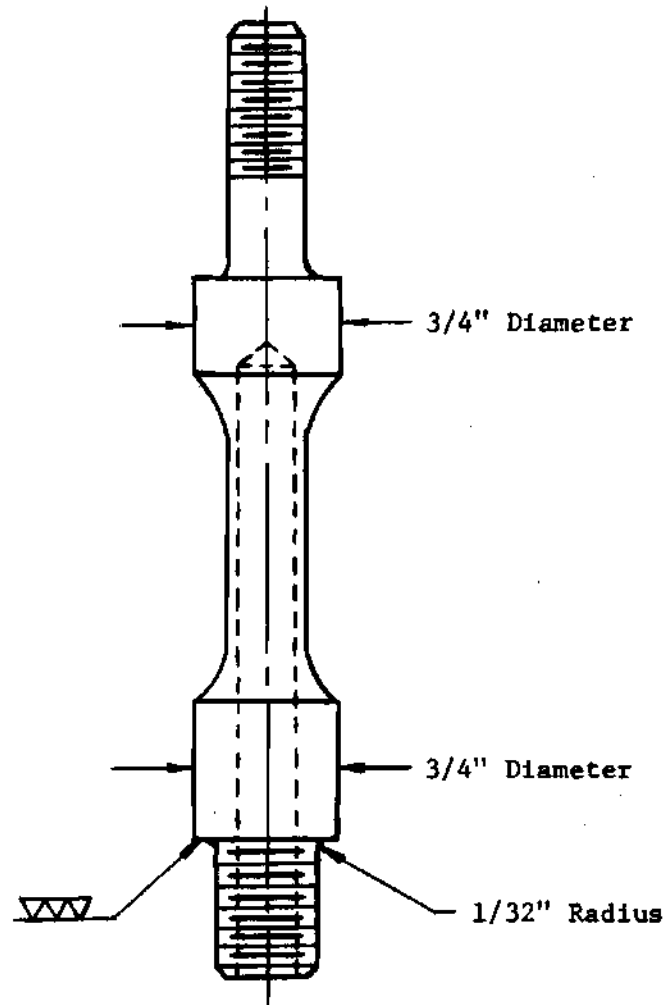


Fig. 24 Specimen Modification.

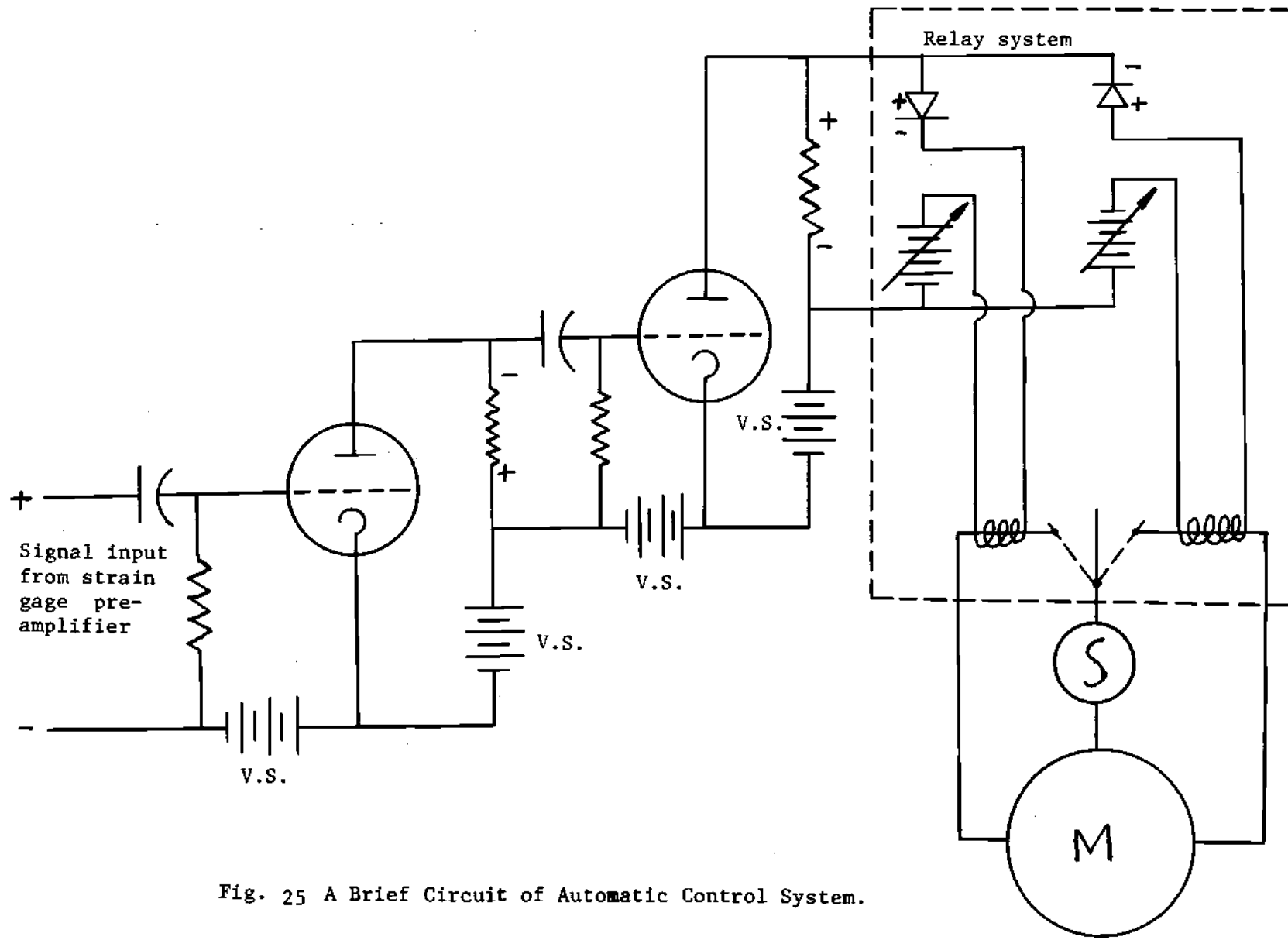


Fig. 25 A Brief Circuit of Automatic Control System.

BIBLIOGRAPHY

1. O. H. Basquin, "The Exponential Law of Endurance Tests", Proceedings, Am. Soc. Testing Mats., Vol. 10, Part II, 1910, pp. 625-630.
2. J. F. Tavernelli and L. F. Coffin, Jr., "Experimental Support for Generalized Equation Predicating Low Cycle Fatigue," Transactions, Am. Soc. Mechanical Engrs., Vol. 84, Series D, 1962, pp. 533-541.
3. JoDean Morrow and F. R. Tuler, "Low Cycle Fatigue Evaluation of Inconel 713C and Waspaloy," Paper No. 64-Met-15, AWS-ASME Metals Engineering Conference, Detroit, Mich., May, 1964.
4. JoDean Morrow, "Cyclic Plastic Strain Energy and Fatigue of Metals," S. T. P. No. 378 published by the American Society for Testing and Materials.
5. Dieter, G. E., "Mechanical Metallurgy," McGraw-Hill, New York, 1961, pp. 54-77.
6. Hans Ziegler, "Principles of Structural Stability," Blaisdell Publishing Company.
7. Bleich, F., "Buckling Strength of Metal Structures," McGraw-Hill, New York, 1952, pp. 1-60.
8. T. L. Boblenz, J. M. Fisher, S. T. Rolfe, and J. H. Gross, "Test Methods for Compression Members," S. T. P. No. 419 published by the American Society for Testing and Materials.
9. J. P. Den Hartog, "Advanced Strength of Materials," New York, McGraw-Hill, 1952.